AIMS Mathematics, 9(4): 10208–10234.
DOI: 10.3934/math.2024499
Received: 05 January 2024
Revised: 13 February 2024
Accepted: 29 February 2024
Published: 14 March 2024

http://www.aimspress.com/journal/Math

Research article

Investigation of SEIR model with vaccinated effects using sustainable fractional approach for low immune individuals

Huda Alsaud[1], Muhammad Owais Kulachi[2], Aqeel Ahmad[2], Mustafa Inc[3,*] and Muhammad Taimoor[2]

[1] Department of Mathematics, College of Science, King Saud University, P.O. Box 22452, Riyadh 11495, Saudi Arabia
[2] Department of Mathematics, Ghazi University, D. G. Khan 32200, Pakistan
[3] Department of Mathematics, Firat University, Elazig 23119, Turkiye

* **Correspondence:** Email: minc@firat.edu.tr.

Abstract: Mathematical formulations are crucial in understanding the dynamics of disease spread within a community. The objective of this research is to investigate the SEIR model of SARS-COVID-19 (C-19) with the inclusion of vaccinated effects for low immune individuals. A mathematical model is developed by incorporating vaccination individuals based on a proposed hypothesis. The fractal-fractional operator (FFO) is then used to convert this model into a fractional order. The newly developed SEVIR system is examined in both a qualitative and quantitative manner to determine its stable state. The boundedness and uniqueness of the model are examined to ensure reliable findings, which are essential properties of epidemic models. The global derivative is demonstrated to verify the positivity with linear growth and Lipschitz conditions for the rate of effects in each sub-compartment. The system is investigated for global stability using Lyapunov first derivative functions to assess the overall impact of vaccination. In fractal-fractional operators, fractal represents the dimensions of the spread of the disease, and fractional represents the fractional ordered derivative operator. We use combine operators to see real behavior of spread as well as control of COVID-19 with different dimensions and continuous monitoring. Simulations are conducted to observe the symptomatic and asymptomatic effects of the corona virus disease with vaccinated measures for low immune individuals, providing insights into the actual behavior of the disease control under vaccination effects. Such investigations are valuable for understanding the spread of the virus and developing effective control strategies based on justified outcomes.

Keywords: mathematical modeling; stability analysis; boundedness; Lipschitz conditions; global derivative
Mathematics Subject Classification: 37C75, 65L03, 65L05, 65L07

1. Introduction

Mathematics was initially utilized in biology in the 13^{th} century by Fibonacci, who developed the famed Fibonacci series to explain an increasing population. Daniel Bernoulli utilized mathematics to describe the impact on tiny shapes. Johannes Reinke coined the phrase "bio maths" in 1901. Biomathematics involves the theoretical examination of mathematical models to understand the principles governing the formation and functioning of biological systems.

Mathematical models are utilized to investigate specific questions related to the studied disease. For example, epidemiological models are important for predicting how infectious diseases spread, and help to control them by identifying important factors in the community. In this case, we want to analyze a particular model to understand how the COVID-19 virus behaves. This virus appeared in late 2019, and continues to be a global challenge. To gain a deeper insight into the underlying physical processes, we delve into the realm of fractional calculus. Previous literature has introduced various operators through the framework of fractional calculus [1, 2]. In the field of C^{η}-Calculus, Golmankhaneh et al. [3] provided an explanation of the Sumudu transform and Laplace transform. Additionally, in 2019, Goyal [4] proposed a fractional model that demonstrated the potential to manage the Lassa hemorrhagic fever disease.

Advancements in technology have led to significant progress in the field of epidemiology, enabling the examination of various infectious diseases for treatment, control, and cure [5]. It is essential to underscore that mathematical biology plays a pivotal role in investigating numerous diseases. Significant strides have been taken in the mathematical modeling of infectious diseases in recent decades, as evidenced by various studies [6, 7]. Over the last thirty years, mathematical modeling has gained prominence in research, making substantial contributions to the development of effective public health strategies for disease control [8, 9]. Mathematical models serve as invaluable tools for analyzing spatiotemporal patterns and the dynamic behavior of infections. Acknowledging their significance, researchers have approached the study of COVID-19 from diverse perspectives in the last three years [10, 11].

Various methodologies have been employed by researchers in this field to devise successful techniques for managing this condition, with recent studies offering additional insights [12, 13]. For example, a recent investigation utilized a mathematical model to evaluate the impacts of immunization in nursing homes [14]. Furthermore, researchers have explored mathematical modeling and effective intervention strategies for controlling the COVID-19 outbreak [15]. Additionally, some studies have delved into COVID-19 mathematical models using stochastic differential equations and environmental white noise [16].

In 2019, China experienced a notable outbreak of the coronavirus disease 2019 (COVID-19), prompting concerns about its potential to escalate into a worldwide pandemic [17]. Researchers from China, particularly Zhao et al., made significant contributions in addressing the challenges posed by COVID-19. This disease is attributed to the severe acute respiratory syndrome coronavirus 2 (SARS-CoV-2), a viral infection. The initial verified case was documented in Wuhan, China, in December 2019 [18]. The infection rapidly spread worldwide, leading to the declaration of a COVID-19 pandemic.

Transmission occurs through various means, including respiratory droplets from coughing, sneezing, close contact, and touching contaminated surfaces. Key preventive measures include

consistent mask usage, frequent hand washing, and maintaining safe interpersonal distances [19]. Effective interventions and real-time data play a crucial role in managing the coronavirus outbreak [20]. Prior studies have employed real-time analysis to comprehend the transmission of the virus among individuals, the severity of the disease, and the early stages of the pathogen, particularly in the initial week of the outbreak [21].

In December 2019, an outbreak of pneumonia cases was reported in Wuhan, initially with unidentified origins. Some cases were associated with exposure to wet markets and seafood. Chinese health authorities, in collaboration with the Chinese Center for Disease Control and Prevention (China CDC), initiated an investigation into the cause and spread of the disease on December 31, 2019 [22]. We conducted an analysis of temporal changes in the outbreak by examining the time interval between hospital admission dates and fatalities. Clinical studies on COVID-19 have indicated that symptoms typically manifest around 7 days after the onset of illness [23]. It is important to consider the duration between hospitalization and death in order to accurately assess the risk of mortality [24]. The information regarding the incubation period of COVID-19 and epidemiological data was sourced from publicly available records of confirmed cases [25].

An established method for the fractional-order model is elaborated upon in [26]. Recent contributions include various fractional models related to COVID-19, such as the analysis by Atangana and Khan focusing on the pandemic's impact on China [27]. Additionally, the COVID-19 model's dynamical aspects were explored using fuzzy Caputo and ABC derivatives, as demonstrated in [28]. A similar type of approach using fractional operator techniques are given in [29–31]. Different author's have investigated the transmission of different infectious disease like COVID-19 with symptomatic and asymptomatic effects in the community by using the fractal-fractional definition [32, 33].

In light of the aforementioned significance, we aim is to address fundamental issues by concentrating on the distinctive challenges posed by the dynamics of COVID-19. To achieve this, we employ a model tailored to accurately capture the characteristics of COVID-19 dynamics and account for the limitations in our response to the pandemic. Initially, we examine the epidemic dynamics within a specific community characterized by a unique social pattern. For this analysis, we adopt a conventional SEIR design that accommodates prolonged incubation periods.

Here, the previous model is given in [34] as follows:

$$\begin{aligned}
\frac{dS}{dt} &= \mathbf{a} - \frac{\rho_1 S I}{1+\gamma I} - (\delta+\rho)S, \\
\frac{dE}{dt} &= \rho S - \delta E - \rho_2 \alpha E I, \\
\frac{dI}{dt} &= \frac{\rho_1 S I}{1+\gamma I} + \rho_2\, \alpha\, E I - (\delta + \mu_0 + \omega - \mathbf{b})\, I, \\
\frac{dR}{dt} &= \omega I - \delta R.
\end{aligned} \tag{1.1}$$

Initial conditions corresponds to the aforementioned system:

$$S^0(t) = S_0,\ E^0(t) = E_0,\ I^0(t) = I_0,\ R^0(t) = R_0.$$

The primary goal of this research is to employ novel fractional derivatives within mathematical analysis and simulation to enhance the COVID-19 model. COVID-19 is a highly dangerous disease that

presents a significant risk to human life. Verification of the existence and distinct characteristics of the solution system is undertaken, coupled with a qualitative assessment of the system. So, we introduce vaccination measures for low immune individuals. We developed new mathematical model by taking vaccination measures which helps to control COVID-19 early which we shall observe on simulation easily. The research involves confirming the presence of a solution system with unique characteristics and conducting a qualitative evaluation of this system. Furthermore, the fractal-fractional derivative is utilized to investigate the real-world behavior of the newly developed mathematical model. Finally, numerical simulations are used to reinforce and authenticate the biological findings.

Definition 1.1. If $0 < \xi \leq 1$ and $0 < \lambda \leq 1$, then the Riemann-Liouville operator for the fractal-fractional Operator (FFO) with a Mittag-Leffler (ML) kernel is defined as $U(t)$ [35].

$$ {}_0^{FFM}D_t^{\xi,\lambda}U(t) = \frac{AB(\xi)}{1-\xi}\int_0^t E_\xi \frac{d\,U(\Omega)}{dt^\lambda}\left[-\frac{\xi}{1-\xi}(t-\Omega)^\xi\right]d\Omega \ , $$

involving $0 < \xi, \ \lambda \leq 1$, and $AB(\xi) = 1 - \xi + \frac{\xi}{\Gamma(\xi)}$.

Therefore, the function $U(t)$, which has an order of (ξ, λ) and a Mittag-Leffler (ML) kernel, is given as follows:

$$ {}_0^{FFM}D_t^{\xi,\lambda}U(t) = \frac{\lambda(1-\xi)t^{\lambda-1}U(t)}{AB(\xi)} + \frac{\xi\lambda}{AB(\xi)}\int_0^t \Omega^{\xi-1}(t-\Omega)U(\Omega)d\Omega \ . $$

2. Formulation of the SEVIR model

A newly developed model for SARS-COVID-19 includes the vaccinated effect, whereas the previous model used the SEIR framework. In this new model, we introduce a new variable called "Vaccinated." With the addition of Vaccinated, the new model is referred to as SEVIR, where "S" represents the Susceptible class, "E" represents the Exposed class, "V" represents the Vaccinated class, "I" represents the Infected class, and "R" represents the Recovered class.

We define several parameters in this model: "**a**" represents the recruitment rate, "δ" represents the death rate due to natural causes, "$\rho + \rho_1$" represents the contact rate from the Susceptible class to the Exposed class, "ρ_2" represents the vaccination rate, "α" represents the rate at which the infection is reducing due to vaccination effects, "μ_0" represents the infection death rate, "ω" represents the rate at which an individual recovers from vaccination and becomes recovered, "**b**" represents the recruitment rate to the Vaccinated class, "ϕ" represents the contact rate from the Vaccinated class to the Infected class, and "ψ" represents the recovery rate.

We want to investigate spread of the SEIR model for SARS-COVID-19 with the vaccinated effect.

So, the flow chart for newly developed model SEVIR is given as Figure 1.

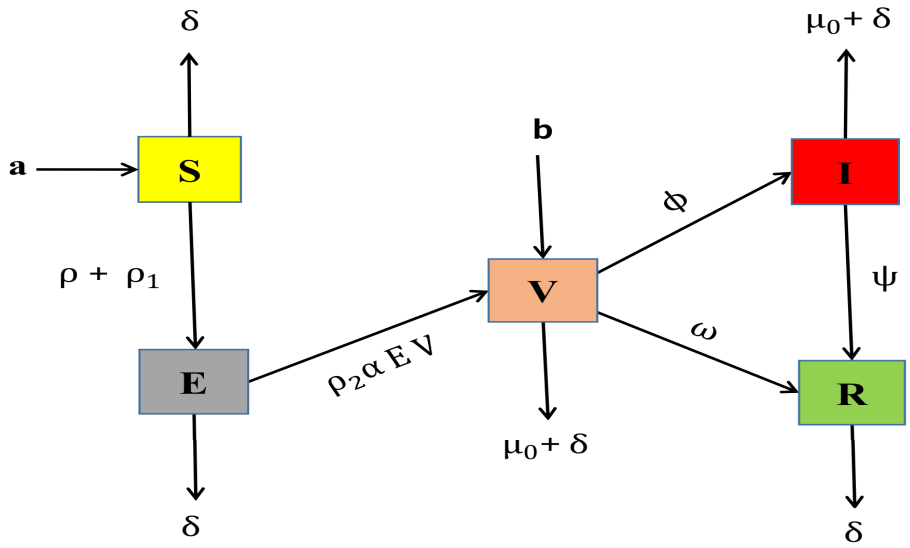

Figure 1. The flow chart illustrates the newly developed model.

The model that was developed based on the generalized hypothesis with the vaccinated effect is presented as follows:

$$\begin{aligned}
\frac{dS}{dt} &= \mathbf{a} - (\delta + \rho + \rho_1)S, \\
\frac{dE}{dt} &= (\rho + \rho_1)S - \delta E - \rho_2 \alpha EV, \\
\frac{dV}{dt} &= \rho_2 \alpha EV - (\delta + \mu_0 + \omega - \mathbf{b} + \phi)V, \\
\frac{dI}{dt} &= \phi V - (\mu_0 + \delta + \psi)I, \\
\frac{dR}{dt} &= \omega V + \psi I - \delta R.
\end{aligned} \tag{2.1}$$

The following are initial conditions linked with the described system:

$$S^0(t) = S_0,\ E^0(t) = E_0,\ V^0(t) = V_0,\ I^0(t) = I_0,\ R^0(t) = R_0.$$

Using the fractal-fractional order (FFO) with a Mittag-Leffler (ML) definition, the above model becomes

$$\begin{aligned}
{}_0^{FFM}D_t^{\xi,\lambda} S(t) &= \mathbf{a} - (\delta + \rho + \rho_1)S, \\
{}_0^{FFM}D_t^{\xi,\lambda} E(t) &= (\rho + \rho_1)S - \delta E - \rho_2 \alpha EV, \\
{}_0^{FFM}D_t^{\xi,\lambda} V(t) &= \rho_2 \alpha EV - (\delta + \mu_0 + \omega - \mathbf{b} + \phi)V, \\
{}_0^{FFM}D_t^{\xi,\lambda} I(t) &= \phi V - (\mu_0 + \delta + \psi)I, \\
{}_0^{FFM}D_t^{\xi,\lambda} R(t) &= \omega V + \psi I - \delta R.
\end{aligned} \tag{2.2}$$

Here, ${}_0^{FFM}D_t^{\xi,\lambda}$ is the fractal-fractional operator with Mittag-Leffler (ML), where $0 < \xi \leq 1$ and $0 < \lambda \leq 1$.

The following are initial conditions linked with the described system:

$$S^0(t) = S_0,\ E^0(t) = E_0,\ V^0(t) = V_0,\ I^0(t) = I_0,\ R^0(t) = R_0.$$

Parameter descriptions are given in the following table.

Parameters	Representation	Reference
a	contact rate from the susceptible to the exposed class	[34]
δ	death rate due to natural causes	[34]
$\rho + \rho_1$	contact rate from the susceptible to the exposed class	[34]
α	rate at which the infection is reducing due to vaccination	[34]
ρ_2	vaccination rate	[34]
μ_0	death rate due to infection	[34]
ω	rate at which an individuals becomes recovered	[34]
b	recruitment rate to the vaccinated class	[34]
ϕ	contact rate from the vaccinated to the infected class	Assumed
ψ	recovery rate	Assumed

2.1. Equilibrium point and reproductive number

For this model, the point of equilibrium without disease (disease free) is

$$D_1(S,\ E,\ V,\ I,\ R) = \left(\frac{\mathbf{a}}{\delta+\rho+\rho_1}, \frac{\mathbf{a}(\rho+\rho_1)}{\delta(\delta+\rho+\rho_1)}, 0, 0, 0\right),$$

as well as the endemic points of equilibrium $D_2(S^*, E^*, V^*, I^*, R^*)$, where

$$\begin{aligned}
S^* &= \frac{\mathbf{a}}{\delta+\rho+\rho_1},\\
E^* &= \frac{-\mathbf{b}+\delta+\phi+\omega+\mu_0}{\alpha\rho_2},\\
V^* &= \frac{(\delta+\psi+\mu_0)\mathbf{A} - \mathbf{b}\delta\rho_1 + \delta^2\rho_1 + \delta\phi\rho_1 + \delta\omega\rho_1 + \delta\mu_0\rho_1 - \mathbf{a}\alpha\rho\rho_2 - \mathbf{a}\alpha\rho_1\rho_2}{\alpha\phi(\mathbf{b}-\delta-\phi-\omega-\mu_0)(\delta+\rho+\rho_1)\rho_2},\\
I^* &= \phi\left(\frac{\mathbf{A} - \mathbf{b}\delta\rho_1 + \delta^2\rho_1 + \delta\phi\rho_1 + \delta\omega\rho_1 + \delta\mu_0\rho_1 - \mathbf{a}\alpha\rho\rho_2 - \mathbf{a}\alpha\rho_1\rho_2}{\alpha(\mathbf{b}-\delta-\phi-\omega-\mu_0)(\delta+\rho+\rho_1)\rho_2}\right),\\
R^* &= (\phi\psi + \delta\omega + \psi\omega + \omega\mu_0) \times \left(\frac{\mathbf{A} - \mathbf{b}\delta\rho_1 + \delta^2\rho_1 + \delta\phi\rho_1 + \delta\omega\rho_1 + \delta\mu_0\rho_1 - \mathbf{a}\alpha\rho\rho_2 - \mathbf{a}\alpha\rho_1\rho_2}{\alpha\delta\phi(\delta+\psi+\mu_0)(\mathbf{b}-\delta-\phi-\omega-\mu_0)(\delta+\rho+\rho_1)\rho_2}\right),
\end{aligned}$$

where

$$\mathbf{A} = -\mathbf{b}\delta^2 + \delta^3 - \mathbf{b}\delta\rho + \delta^2\rho + \delta^2\phi + \delta\rho\phi + \delta^2\omega + \delta\rho\omega + \delta^2\mu_0 + \delta\rho\mu_0.$$

The reproductive number for the newly developed system by using the next generation method is

$$R_0 = \frac{\mathbf{b}\delta(\delta+\rho+\rho_1) + \mathbf{a}\alpha\rho_2(\rho+\rho_1)}{\delta(\delta+\rho+\rho_1)(\delta+\phi+\omega+\mu_0)}.$$

3. Bounded and positive solutions

In this section, we demonstrate the boundedness and positivity of the developed model.

Theorem 3.1. The considered initial condition is

$$\{S_0, E_0, V_0, I_0, R_0\} \subset \Upsilon,$$

and therefore the solutions $\{S, E, V, I, R\}$ will be positive $\forall$ t ≥ 0.

Proof. We will begin the primary analysis to show the improved quality of the solutions. These solutions effectively address real-world issues and have positive outcomes. We will follow the methodology provided in references [36–38]. In this segment, we will examine the conditions required to ensure positive outcomes from the proposed model. To accomplish this, we will establish a standard.

$$\| \beta \|_\infty = \sup_{t \in D_\beta} | \beta(t) |,$$

where "D_β" represents the β domain. Now, we continue with $S(t)$.

$$\begin{aligned} {}_0^{FFM}D_t^{\xi,\lambda} S(t) &= \mathbf{a} - (\delta + \rho + \rho_1)S, \quad \forall t \geq 0, \\ &\geq -(\delta + \rho + \rho_1)\, S, \quad \forall t \geq 0. \end{aligned}$$

This yield

$$S(t) \geq S(0)E_\xi\Big[- \frac{c^{1-\lambda}\xi(\delta + \rho + \rho_1)t^\xi}{AB(\xi) - (1-\xi)(\delta + \rho + \rho_1)}\Big], \quad \forall t \geq 0,$$

where "c" represents the time element. This demonstrates that the $S(t)$ individuals must be positive $\forall\ t \geq 0$. Now, we have the $E(t)$ individuals as follows:

$$\begin{aligned} {}_0^{FFM}D_t^{\xi,\lambda} E(t) &= (\rho + \rho_1)S - \delta E - \rho_2 \alpha E V, \quad \forall\ t \geq 0, \\ &\geq -(\delta + \rho_2\alpha \mid V \mid)E, \quad \forall\ t \geq 0, \\ &\geq -(\delta + \rho_2\alpha \sup_{t \in D_V} \mid V \mid)E, \quad \forall\ t \geq 0, \\ &\geq -(\delta + \rho_2\alpha \| V \|_\infty)E, \quad \forall\ t \geq 0. \end{aligned}$$

This yield

$$E(t) \geq E(0)E_\xi\Big[- \frac{c^{1-\lambda}\xi(\delta + \rho_2\alpha \| V \|_\infty)t^\xi}{AB(\xi) - (1-\xi)(\delta + \rho_2\alpha \| V \|_\infty)}\Big], \quad \forall\ t \geq 0,$$

where "c" represents the time element. This demonstrates that the $E(t)$ individuals must be positive $\forall\ t \geq 0$. Now, we have the $V(t)$ individuals as follows:

$$\begin{aligned} {}_0^{FFM}D_t^{\xi,\lambda} V(t) &= \rho_2\alpha E I - (\delta + \mu_0 + \omega - \mathbf{b} + \phi)V, \quad \forall t \geq 0, \\ &\geq -(-\rho_2\alpha \mid E \mid + \mu_0 + \delta + \omega - \mathbf{b} + \phi)V, \quad \forall t \geq 0, \\ &\geq -(-\rho_2\alpha \sup_{t \in D_E} \mid E \mid + \mu_0 + \delta + \omega - \mathbf{b} + \phi)V, \quad \forall t \geq 0, \\ &\geq -(-\rho_2\alpha \| E \|_\infty + \mu_0 + \delta + \omega - \mathbf{b} + \phi)V, \quad \forall t \geq 0. \end{aligned}$$

This yield

$$V(t) \geq V(0)E_{\xi}\Big[- \frac{c^{1-\lambda\xi}(-\rho_2\alpha \parallel E \parallel_{\infty} +\mu_0 + \delta + \omega - \mathbf{b} + \phi)t^{\xi}}{AB(\xi) - (1-\xi)\,(-\rho_2\alpha \parallel E \parallel_{\infty} +\mu_0 + \delta + \omega - \mathbf{b} + \phi)}\Big], \quad \forall t \geq 0,$$

where "c" represents the time element. This demonstrates that the $V(t)$ individuals must be positive $\forall\ t \geq 0$. Now, we have the $I(t)$ individuals as follows:

$$\begin{aligned} {}_0^{FFM}D_t^{\xi,\lambda}I(t) &= \phi V - (\mu_0 + \delta + \psi)I, \quad \forall t \geq 0, \\ &\geq -(\mu_0 + \delta + \psi)I(t), \quad \forall t \geq 0. \end{aligned}$$

This yield

$$I(t) \geq I(0)E_{\xi}\Big[- \frac{c^{1-\lambda}\xi(\mu_0 + \delta + \psi)t^{\xi}}{AB(\xi) - (1-\xi)(\mu_0 + \delta + \psi)}\Big], \quad \forall t \geq 0,$$

where "c" represents the time element. This demonstrates that the $I(t)$ individuals must be positive $\forall\ t \geq 0$. Now, we have the $R(t)$ individuals as follows:

$$\begin{aligned} {}_0^{FFM}D_t^{\xi,\lambda}R(t) &= \omega V + \psi I - \delta R, \quad \forall\, t \geq 0, \\ &\geq -(\delta)R(t), \quad \forall\, t \geq 0. \end{aligned}$$

This yield

$$R(t) \geq R(0)E_{\xi}\Big[- \frac{c^{1-\lambda}\xi(\delta)t^{\xi}}{AB(\xi) - (1-\xi)(\delta)}\Big], \quad \forall t \geq 0,$$

where "c" represents the time element. This demonstrates that the $R(t)$ individuals must be positive $\forall\ t \geq 0$.

Theorem 3.2. Solutions of our developed model given in Eq (2.2) with positive initial values are all bounded.

Proof. The above theorem demonstrates that the solutions of our developed model must be positive $\forall\ t \geq 0$, and the strategies are described in [39]. Because $X = S + E + V$, then

$${}_0^{FFM}D_t^{\xi,\lambda}X(t) = \mathbf{a} - \delta X - (\mu_0 + \omega - \mathbf{b} + \phi)V.$$

We achieved as follows:

$$\Psi_p = \{S, \quad E, \quad V \in R_+^3 \mid S + V \leq X\} \quad \forall\ t \geq 0.$$

Further we have X_{υ}=I+R. So, we have

$${}_0^{FFM}D_t^{\xi,\lambda}X_{\upsilon}(t) = (\phi + \omega)V - \mu_0 I - X_{\upsilon}\delta.$$

Upon solving the above equation and taking $t \to \infty$,we get

$$X_{\upsilon} \leq \frac{(\phi + \omega)V - \mu_0 I}{\delta}.$$

Thus,

$$\Psi_{\upsilon} = \left\{ I,\ R \in R_{+}^{2} \mid X_{\upsilon} \leq \frac{(\phi + \omega)I - \mu_0 Q}{\delta} \right\} \quad \forall\ t \geq 0.$$

The model's mathematical solutions (2.2) are confined to the region Ψ.

$$\Psi = \left\{ S,\ E,\ V,\ I,\ R \in R_{+}^{5} \mid S + V \leq X, X_{\upsilon} \leq \frac{(\phi + \omega)V - \mu_0 I}{\delta} \right\} \quad \forall\ t \geq 0.$$

This demonstrates that for every $t \geq 0$, all solutions remain positive, consistent with the provided initial conditions in the domain Ψ.

Theorem 3.3. The proposed coronavirus model (2.2) in R_{+}^{5} has positive invariant solutions, in addition to the initial conditions.

Proof. In this particular scenario, we applied the procedure described in [40]. We have

$$\begin{aligned}
{}_{0}^{FFM}D_{t}^{\xi,\lambda}(S(t))_{S=0} &= \mathbf{a} \quad \geq 0, \\
{}_{0}^{FFM}D_{t}^{\xi,\lambda}(E(t))_{E=0} &= (\rho + \rho_1)S \quad \geq 0, \\
{}_{0}^{FFM}D_{t}^{\xi,\lambda}(V(t))_{V=0} &= \rho_2 \alpha E V + \mathbf{b}V \quad \geq 0, \\
{}_{0}^{FFM}D_{t}^{\xi,\lambda}(I(t))_{I=0} &= \phi V \quad \geq 0, \\
{}_{0}^{FFM}D_{t}^{\xi,\lambda}(R(t))_{R=0} &= \omega V + \psi I \quad \geq 0.
\end{aligned} \tag{3.1}$$

If $(S_0, E_0, V_0, I_0, R_0) \in R_{+}^{5}$, then our obtained solution is unable to escape from the hyperplane, as stated in Eq (3.1). This proves that the R_{+}^{5} domain is positive invariant.

4. Impact of global derivatives for uniqueness and existence of solutions

The Riemann-Stieltjes integral has been widely recognized in the literature as the most commonly used integral. If

$$Y(x) = \int y(x)dx,$$

then the Riemann-Stieltjes integral is given as follows:

$$Y_{w}(x) = \int y(x)dw(x),$$

where the $y(x)$ global derivative with respect to $w(x)$ is

$$D_{w}y(x) = \lim_{h \to 0} \frac{y(x+h) - y(x)}{w(x+h) - w(x)}.$$

If the above function's numerator and denominator are differentiated, we get

$$D_{w}y(x) = \frac{y^{'}(x)}{w^{'}(x)},$$

assuming that $w^{'}(x) \neq 0$, $\forall x \in D_{w'}$. Now, we will test the impact on the coronavirus by using the global derivative instead of the classical derivative:

$$\begin{aligned} D_w S &= \mathbf{a} - (\delta + \rho + \rho_1)S, \\ D_w E &= (\rho + \rho_1)S - \delta E - \rho_2 \alpha E V, \\ D_w V &= \rho_2 \alpha E V - (\delta + \mu_0 + \omega - \mathbf{b} + \phi)V, \\ D_w I &= \phi V - (\mu_0 + \delta + \psi)I, \\ D_w R &= \omega V + \psi I - \delta R. \end{aligned}$$

For the sake of clean notation, we shall suppose that w is differentiable.

$$\begin{aligned} S^{'} &= w^{'}[\mathbf{a} - (\delta + \rho + \rho_1)S], \\ E^{'} &= w^{'}[(\rho + \rho_1)S - \delta E - \rho_2 \alpha E V], \\ V^{'} &= w^{'}[\rho_2 \alpha E V - (\delta + \mu_0 + \omega - \mathbf{b} + \phi)V], \\ I^{'} &= w^{'}[\phi V - (\mu_0 + \delta + \psi)I], \\ R^{'} &= w^{'}[\omega V + \psi I - \delta R]. \end{aligned}$$

An appropriate choice of the function $w(t)$ will lead to a specific outcome. For instance, if $w(t) = t^{\alpha}$, where α is a real number, we will observe fractal movement. We had to take action due to the circumstances that

$$\| w^{'} \|_{\infty} = \sup_{t \in D_{w'}} | w^{'}(t) | < N.$$

The below example demonstrates the unique solution for the developed system:

$$\begin{aligned} S^{'} &= w^{'}[\mathbf{a} - (\delta + \rho + \rho_1)S] = Z_1(t, S, G), \\ E^{'} &= w^{'}[(\rho + \rho_1)S - \delta E - \rho_2 \alpha E V] = Z_2(t, S, G), \\ V^{'} &= w^{'}[\rho_2 \alpha E V - (\delta + \mu_0 + \omega - \mathbf{b} + \phi)V] = Z_3(t, S, G), \\ I^{'} &= w^{'}[\phi V - (\mu_0 + \delta + \psi)I] = Z_4(t, S, G), \\ R^{'} &= w^{'}[\omega V + \psi I - \delta R] = Z_5(t, S, G), \end{aligned}$$

where $G = E, V, I, R$.

We need to confirm the first two requirements as follows:

(1) $| Z(t, S, G) |^2 < K(1 + | S |^2$,

(2) $\forall\, S_1, S_2$, we have, $\| Z(t, S_1, G) - Z(t, S_2, G) \|^2 < \bar{K} \| S_1 - S_2 \|_{\infty}^2$.

Initially,

$$\begin{aligned} | Z_1(t, S, G) |^2 &= | w^{'}[\mathbf{a} - (\delta + \rho + \rho_1)S] |^2, \\ &= | w^{'}[\mathbf{a} + (-\delta - \rho - \rho_1)S] |^2, \\ &\leq 2 | w^{'} |^2 \left(\mathbf{a}^2 + | (-\delta - \rho - \rho_1)S |^2\right), \\ &\leq 2 \sup_{t \in D_{w'}} | w^{'} |^2 \mathbf{a}^2 + 6 \sup_{t \in D_{w'}} | w^{'} |^2 \left(\rho^2 + \delta^2 + \rho_1\right) | S |^2, \end{aligned}$$

$$\begin{aligned}
&\leq 2 \parallel w^{'} \parallel_{\infty}^{2} \mathbf{a}^{2} + 6 \parallel w^{'} \parallel_{\infty}^{2} \left(\rho^{2} + \delta^{2} + \rho_{1}^{2}\right) \mid S \mid^{2}, \\
&\leq 2 \parallel w^{'} \parallel_{\infty}^{2} \mathbf{a}^{2} \left(1 + \frac{3}{\mathbf{a}^{2}}(\rho^{2} + \delta^{2} + \rho_{1}^{2}) \mid S \mid^{2}\right), \\
&\leq K_{1}(1 + \mid S \mid^{2}),
\end{aligned}$$

under the condition

$$\frac{3}{\mathbf{a}^{2}}(\rho^{2} + \delta^{2} + \rho_{1}^{2}) < 1,$$

involving

$$K_{1} = 2 \parallel w^{'} \parallel_{\infty}^{2} \mathbf{a}^{2}.$$

$$\begin{aligned}
\mid Z_{2}(t, S, G) \mid^{2} &= \mid w^{'}[(\rho + \rho_{1})S - \delta E - \rho_{2}\alpha E V] \mid^{2}, \\
&= \mid w^{'}[(\rho + \rho_{1})S + (-\delta - \rho_{2}\alpha V)E] \mid^{2}, \\
&\leq 2 \mid w^{'} \mid^{2} \left(\mid (\rho + \rho_{1})S \mid^{2} + (-\delta - \rho_{2}\alpha V)E \mid^{2}\right), \\
&\leq 4 \sup_{t \in D_{w^{'}}} \mid w^{'} \mid^{2} (\rho^{2} + \rho_{1}^{2}) \sup_{t \in D_{S}} \mid S \mid^{2} + 4 \sup_{t \in D_{w^{'}}} \mid w^{'} \mid^{2} (\delta^{2} + \rho_{2}^{2}\alpha^{2} \sup_{t \in D_{V}} \mid V \mid^{2}) \mid E \mid^{2}, \\
&\leq 4 \parallel w^{'} \parallel_{\infty}^{2} (\rho^{2} + \rho_{1}^{2}) \parallel S \parallel_{\infty}^{2} + 4 \parallel w^{'} \parallel_{\infty}^{2} (\delta^{2} + \rho_{2}^{2}\alpha^{2} \parallel V \parallel_{\infty}^{2}) \mid E \mid^{2}, \\
&\leq 4 \parallel w^{'} \parallel_{\infty}^{2} (\rho^{2} + \rho_{1}^{2}) \parallel S \parallel_{\infty}^{2} \left(1 + \frac{(\delta^{2} + \rho_{2}^{2}\alpha^{2} \parallel V \parallel_{\infty}^{2}) \mid E \mid^{2}}{(\rho^{2} + \rho_{1}^{2}) \parallel S \parallel_{\infty}^{2}}\right), \\
&\leq K_{2}(1 + \mid E \mid^{2}),
\end{aligned}$$

under the condition

$$\frac{(\delta^{2} + \rho_{2}^{2}\alpha^{2} \parallel V \parallel_{\infty}^{2})}{(\rho^{2} + \rho_{1}^{2}) \parallel S \parallel_{\infty}^{2}} < 1,$$

where

$$K_{2} = 2 \parallel w^{'} \parallel_{\infty}^{2} (\rho^{2} + \rho_{1}^{2}) \parallel S \parallel_{\infty}^{2}.$$

$$\begin{aligned}
\mid Z_{3}(t, S, G) \mid^{2} &= \mid w^{'}[\rho_{2}\alpha E V - (\delta + \mu_{0} + \omega - \mathbf{b} + \phi)V] \mid^{2}, \\
&= \mid w^{'}[\rho_{2}\alpha E V + \mathbf{b}V + (-\delta - \mu_{0} - \omega - \phi)V] \mid^{2}, \\
&\leq 2 \mid w^{'} \mid^{2} \left(\mid \rho_{2}\alpha E + \mathbf{b} \mid^{2} + \mid (-\delta - \mu_{0} - \omega - \phi) \mid^{2}\right) \mid V \mid^{2}, \\
&\leq 4 \sup_{t \in D_{w^{'}}} \mid w^{'} \mid^{2} [(\rho_{2}^{2}\alpha^{2} \sup_{t \in D_{E}} \mid E \mid^{2} + \mathbf{b}^{2}) + 2(\delta^{2} + \mu_{0}^{2} + \omega^{2} + \phi^{2})] \mid V \mid^{2}, \\
&\leq 4 \parallel\mid w^{'} \parallel_{\infty}^{2} \left[(\rho_{2}^{2}\alpha^{2} \parallel E \parallel_{\infty}^{2} + \mathbf{b}^{2}) + 2(\delta^{2} + \mu_{0}^{2} + \omega^{2} + \phi^{2})\right] \mid V \mid^{2}, \\
&\leq 4 \parallel\mid w^{'} \parallel_{\infty}^{2} (\rho_{2}^{2}\alpha^{2} \parallel E \parallel_{\infty}^{2} + \mathbf{b}^{2}) \left[1 + \frac{2(\delta^{2} + \mu_{0}^{2} + \omega^{2} + \phi^{2})}{\left(\rho_{2}^{2}\alpha^{2} \parallel E \parallel_{\infty}^{2} + \mathbf{b}^{2}\right)}\right] \mid V \mid^{2}, \\
&\leq K_{3}(2 \mid V \mid^{2}),
\end{aligned}$$

under the condition

$$\frac{2(\delta^2+\mu_0^2+\omega^2+\phi^2)}{\left(\rho_2^2\alpha^2 \parallel E \parallel_\infty^2 +\mathbf{b}^2\right)} \leq 1,$$

where

$$K_3 = 4 \parallel\mid w^{'} \parallel_\infty^2 (\rho_2^2\alpha^2 \parallel E \parallel_\infty^2 +\mathbf{b}^2).$$

$$\begin{aligned}
\mid Z_4(t,S,G) \mid^2 &= \mid w^{'}[\phi V-(\mu_0+\delta+\psi)I] \mid^2,\\
&= \mid w^{'}[\phi V+(-\mu_0-\delta-\psi)I] \mid^2,\\
&\leq 2 \mid w^{'} \mid^2 \left(\mid \phi V \mid^2 + \mid (-\mu_0-\delta-\psi)I \mid^2\right),\\
&\leq 2 \sup_{t\in D_{w^{'}}} \mid w^{'} \mid^2 \phi^2 \sup_{t\in D_V} \mid V \mid^2 +6 \sup_{t\in D_{w^{'}}} \mid w^{'} \mid^2 (\mu_0^2+\delta^2+\psi^2) \mid I \mid^2,\\
&\leq 2 \parallel w^{'} \parallel_\infty^2 \phi^2 \parallel V \parallel_\infty^2 +6 \parallel w^{'} \parallel_\infty^2 (\mu_0^2+\delta^2+\psi^2) \mid I \mid^2,\\
&\leq 2 \parallel w^{'} \parallel_\infty^2 \phi^2 \parallel I \parallel_\infty^2 \left(1+\frac{3(\mu_0^2+\delta^2+\psi^2) \mid I \mid^2}{\phi^2 \parallel I \parallel_\infty^2}\right),\\
&\leq K_4(1+\mid I \mid^2),
\end{aligned}$$

under the condition

$$\frac{3(\mu_0^2+\delta^2+\psi^2)}{\phi^2 \parallel V \parallel_\infty^2} < 1,$$

where

$$K_4 = 2 \parallel w^{'} \parallel_\infty^2 \phi^2 \parallel V \parallel_\infty^2 .$$

$$\begin{aligned}
\mid Z_5(t,S,G) \mid^2 &= \mid w^{'}[\omega V+\psi I-\delta R] \mid^2,\\
&= \mid w^{'}[(\omega V+\psi I)+(-\delta R)] \mid^2,\\
&\leq 2 \mid w^{'} \mid^2 \left(\mid (\omega V+\psi I) \mid^2 + \mid -\delta R \mid^2\right),\\
&\leq 4 \sup_{t\in D_{w^{'}}} \mid w^{'} \mid^2 \left(\omega^2 \sup_{t\in D_V} \mid V \mid^2 +\psi \sup_{t\in D_I} \mid I \mid^2\right) + 2 \sup_{t\in D_{w^{'}}} \mid w^{'} \mid^2 \delta^2 \mid R \mid^2,\\
&\leq 4 \parallel w^{'} \parallel_\infty^2 \left(\omega^2 \parallel V \parallel_\infty^2 +\psi \parallel I \parallel_\infty^2\right) + 2 \parallel w^{'} \parallel_\infty^2 \delta^2 \mid R \mid^2),\\
&\leq 4 \parallel w^{'} \parallel_\infty^2 (\omega^2 \parallel V \parallel_\infty^2 +\psi^2 \parallel I \parallel_\infty^2)\left(1+\frac{\delta^2 \mid R \mid^2}{2(\omega^2 \parallel V \parallel_\infty^2 +\psi^2 \parallel I \parallel_\infty^2)}\right),\\
&\leq K_5(1+\mid R \mid^2),
\end{aligned}$$

under the condition

$$\frac{\delta^2}{2(\omega^2 \parallel V \parallel_\infty^2 +\psi^2 \parallel I \parallel_\infty^2)} < 1,$$

where

$$K_5 = 4 \parallel w^{'} \parallel_{\infty}^2 (\omega^2 \parallel V \parallel_{\infty}^2 + \psi^2 \parallel I \parallel_{\infty}^2).$$

Hence the linear growth condition is satisfied.

Further, we validate the Lipschitz condition.

If

$$\begin{aligned}
| Z_1(t, S_1, G) - Z_1(t, S_2, G) |^2 &= | w^{'}(-\delta - \rho - \rho_1)(S_1 - S_2) |^2, \\
| Z_1(t, S_1, G) - Z_1(t, S_2, G) |^2 &\leq | w^{'} |^2 (3\delta^2 + 3\rho^2 + 3\rho_1^2) | S_1 - S_2 |^2, \\
\sup_{t \in D_S} | Z_1(t, S_1, G) - Z_1(t, S_2, G) |^2 &\leq \sup_{t \in D_{w'}} | w^{'} |^2 \left(3\delta^2 + 3\rho^2 + 3\rho_1^2\right) \sup_{t \in D_S} | S_1 - S_2 |^2, \\
\parallel Z_1(t, S_1, G) - Z_1(t, S_2, G) \parallel_{\infty}^2 &\leq \parallel w^{'} \parallel_{\infty}^2 (3\delta^2 + 3\rho^2 + 3\rho_1^2) \parallel S_1 - S_2 \parallel_{\infty}^2, \\
\parallel Z_1(t, S_1, G) - Z_1(t, S_2, G) \parallel_{\infty}^2 &\leq \bar{K_1} \parallel S_1 - S_2 \parallel_{\infty}^2,
\end{aligned}$$

where

$$\bar{K_1} = \parallel w^{'} \parallel_{\infty}^2 \left(3\delta^2 + 3\rho^2 + 3\rho_1^2\right).$$

If

$$\begin{aligned}
| Z_2(t,\ S,\ E_1,\ V,\ I,\ R) - Z_2(t,\ S,\ E_2,\ V,\ I,\ R) |^2 &= | w^{'}(-\delta - \rho_2 \alpha V)(E_1 - E_2) |^2, \\
| Z_2(t,\ S,\ E_1,\ V,\ I,\ R) - Z_2(t,\ S,\ E_2,\ V,\ I,\ R) |^2 &\leq | w^{'} |^2 (2\delta^2 + 2\rho_2^2 \alpha^2 | V |^2) | E_1 - E_2 |^2, \\
\sup_{t \in D_E} | Z_2(t,\ S,\ E_1,\ V,\ I,\ R) - Z_2(t,\ S,\ E_2,\ V,\ I,\ R) |^2 &\leq \sup_{t \in D_{w'}} | w^{'} |^2 (2\delta^2 + 2\rho_2^2 \alpha^2 \sup_{t \in D_V} | V |^2) \sup_{t \in D_E} \\
&\quad \times | E_1 - E_2 |^2, \\
\parallel Z_2(t,\ S,\ E_1,\ V,\ I,\ R) - Z_2(t,\ S,\ E_2,\ V,\ I,\ R) \parallel_{\infty}^2 &\leq \parallel w^{'} \parallel_{\infty}^2 (2\delta^2 + 2\rho_2^2 \alpha^2 \parallel V \parallel_{\infty}^2), \parallel E_1 - E_2 \parallel_{\infty}^2, \\
\parallel Z_2(t,\ S,\ E_1,\ V,\ I,\ R) - Z_2(t,\ S,\ E_2,\ V,\ I,\ R) \parallel_{\infty}^2 &\leq \bar{K_2} \parallel E_1 - E_2 \parallel_{\infty}^2,
\end{aligned}$$

where

$$\bar{K_2} = \parallel w^{'} \parallel_{\infty}^2 (2\delta^2 + 2\rho_2^2 \alpha^2 \parallel V \parallel_{\infty}^2).$$

If

$$\begin{aligned}
&| Z_3(t,\ S,\ E,\ V_1,\ I,\ R) - Z_3(t,\ S,\ E,\ V_2,\ I,\ R) |^2 \\
= \ &| w^{'} (\rho_2 \alpha E + \mathbf{b} + (-\delta - \mu_0 - \omega - \phi)) (V_1 - V_2) |^2,
\end{aligned}$$

$$\begin{aligned}
&| Z_3(t,\ S,\ E,\ V_1,\ I,\ R) - Z_3(t,\ S,\ E,\ V_2,\ I,\ R) |^2 \\
\leq \ &2 | w^{'} |^2 \left(| \rho_2 \alpha E + \mathbf{b} |^2 + | (-\delta - \mu_0 - \omega - \phi) |^2 \right) \\
&\times | V_1 - V_2 |^2,
\end{aligned}$$

$$\begin{aligned}
\sup_{t\in D_V} \mid Z_3(t,\ S,\ E,\ V_1,\ I,\ R) - Z_3(t,\ S,\ E,\ V_2,\ I,\ R) \mid^2 &\leq 4 \sup_{t\in D_{w'}} \mid w^{'} \mid^2 \Big(\rho_2^2\alpha^2 \sup_{t\in D_E} \mid E \mid^2 + \mathbf{b}^2 \\
&\quad +2(\delta^2+\mu_0^2+\omega^2+\phi^2)\Big) \sup_{t\in D_V} \mid V_1 - V_2 \mid^2, \\
\| Z_3(t,\ S,\ E,\ V_1,\ I,\ R) - Z_3(t,\ S,\ E,\ V_2,\ I,\ R) \|_\infty^2 &\leq 4 \| w^{'} \|_\infty^2 \Big(\rho_2^2\alpha^2 \| E \|_\infty^2 + \mathbf{b}^2 \\
&\quad +2(\delta^2+\mu_0^2+\omega^2+\phi^2)\Big) \| V_1 - V_2 \|_\infty^2, \\
\| Z_3(t,\ S,\ E,\ V_1,\ I,\ R) - Z_3(t,\ S,\ E,\ V_2,\ I,\ R) \|_\infty^2 &\leq \bar{K}_3 \| V_1 - V_2 \|_\infty^2,
\end{aligned}$$

where

$$\bar{K}_3 = 4 \| w^{'} \|_\infty^2 \Big(\rho_2^2\alpha^2 \| E \|_\infty^2 + \mathbf{b}^2 + 2(\delta^2+\mu_0^2+\omega^2+\phi^2)\Big).$$

If

$$\begin{aligned}
\mid Z_4(t,\ S,\ E,\ V,\ I_1,\ R) - Z_4(t,\ S,\ E,\ V,\ I_2,\ R) \mid^2 &= \mid w^{'}(-\mu_0-\delta-\psi)](Q_1-Q_2) \mid^2, \\
\mid Z_4(t,\ S,\ E,\ V,\ I_1,\ R) - Z_4(t,\ S,\ E,\ V,\ I_2,\ R) \mid^2 &= \mid w^{'} \mid^2 (3\mu_0^2+3\delta^2+3\psi^2) \mid I_1 - I_2 \mid^2, \\
\sup_{t\in D_I} Z_4(t,\ S,\ E,\ V,\ I_1,\ R) - Z_4(t,\ S,\ E,\ V,\ I_2,\ R) \mid^2 &= \sup_{t\in D_{w'}} \mid w^{'} \mid^2 (3\mu_0^2+3\delta^2+3\psi^2) \sup_{t\in D_I} \mid I_1 - I_2 \mid^2, \\
\| Z_4(t,\ S,\ E,\ V,\ I_1,\ R) - Z_4(t,\ S,\ E,\ V,\ I_2,\ R) \|_\infty^2 &\leq \| w^{'} \|_\infty^2 (3\mu_0^2+3\delta^2+3\psi^2) \| I_1 - I_2 \|_\infty^2, \\
\| Z_4(t,\ S,\ E,\ V,\ I_1,\ R) - Z_4(t,\ S,\ E,\ V,\ I_2,\ R) \|_\infty^2 &\leq \bar{K}_4 \| I_1 - I_2 \|_\infty^2,
\end{aligned}$$

where

$$\bar{K}_4 = \| w^{'} \|_\infty^2 (3\mu_0^2+3\delta^2+3\psi^2).$$

If

$$\begin{aligned}
\mid Z_5(t,\ S,\ E,\ V,\ I,\ R_1) - Z_5(t,\ S,\ E,\ V,\ I,\ R_2) \mid^2 &= \mid w^{'}(-\delta)(R_1-R_2) \mid^2, \\
\mid Z_5(t,\ S,\ E,\ V,\ I,\ R_1) - Z_5(t,\ S,\ E,\ V,\ I,\ R_2) \mid^2 &\leq \mid w^{'} \mid^2 \delta^2 \mid (R_1-R_2) \mid^2, \\
\sup_{t\in D_R} \mid Z_5(t,\ S,\ E,\ V,\ I,\ R_1) - Z_5(t,\ S,\ E,\ V,\ I,\ R_2) \mid^2 &\leq \sup_{t\in D_{w'}} \mid w^{'} \mid^2 \delta^2 \sup_{t\in D_R} \mid R_1 - R_2 \mid^2, \\
\| Z_5(t,\ S,\ E,\ V,\ I,\ R_1) - Z_5(t,\ S,\ E,\ V,\ I,\ R_2) \|_\infty^2 &\leq \| w^{'} \|_\infty^2 \delta^2 \| R_1 - R_2 \|_\infty^2, \\
\| Z_5(t,\ S,\ E,\ V,\ I,\ R_1) - Z_5(t,\ S,\ E,\ V,\ I,\ R_2) \|_\infty^2 &\leq \bar{K}_5 \| R_1 - R_2 \|_\infty^2,
\end{aligned}$$

involving

$$\bar{K}_5 = \| w^{'} \|_\infty^2 \delta^2.$$

Then, given the condition, system (2.2) has a particular solution.

$$\max\Big[\frac{3}{\mathbf{a}^2}(\rho^2+\delta^2+\rho_1^2), \frac{(\delta^2+\rho_2^2\alpha^2 \| V \|_\infty^2)}{(\rho^2+\rho_1^2) \| S \|_\infty^2}, \frac{2(\delta^2+\mu_0^2+\omega^2+\phi^2)}{\Big(\rho_2^2\alpha^2 \| E \|_\infty^2 + \mathbf{b}^2\Big)}, \frac{3(\mu_0^2+\delta^2+\psi^2)}{\phi^2 \| V \|_\infty^2}, \frac{\delta^2}{2(\omega^2 \| V \|_\infty^2 + \psi^2 \| I \|_\infty^2)}\Big] < 1.$$

5. Global stability for developed system

We use Lyapunov's approach and LaSalle's concept of invariance to analyze global stability and determine the conditions for eliminating diseases.

5.1. Lyapunov's first derivative

Theorem 5.1. [41] When the reproductive number $R_0 > 1$, the endemic equilibrium points of the SEVIR model are globally asymptotically stable.

Proof. The Lyapunov function can be expressed in the following manner:

$$\begin{aligned} L(S^*, E^*, V^*, I^*, R^*) &= \left(S - S^* - S^* \log \frac{S}{S^*}\right) + \left(E - E^* - E^* \log \frac{E}{E^*}\right) + \left(V - V^* - V^* \log \frac{V}{V^*}\right) \\ &\quad + \left(I - I^* - I^* \log \frac{I}{I^*}\right) + \left(R - R^* - R^* \log \frac{R}{R^*}\right). \end{aligned}$$

By applying a derivative on both sides,

$$D_t^{\xi,\lambda} L = \dot{L} = \left(\frac{S - S^*}{S}\right) D_t^{\xi,\lambda} S + \left(\frac{E - E^*}{E}\right) D_t^{\xi,\lambda} E + \left(\frac{V - V^*}{V}\right) D_t^{\xi,\lambda} V + \left(\frac{I - I^*}{I}\right) D_t^{\xi,\lambda} I + \left(\frac{R - R^*}{R}\right) D_t^{\xi,\lambda} R,$$

we get

$$\begin{aligned} D_t^{\xi,\lambda} L &= \left(\frac{S - S^*}{S}\right)(\mathbf{a} - (\delta + \rho + \rho_1)S) + \left(\frac{E - E^*}{E}\right)((\rho + \rho_1)S - \delta E - \rho_2 \alpha E V) + \left(\frac{V - V^*}{V}\right) \\ &\quad \times (\rho_2 \alpha E V - (\delta + \mu_0 + \omega - \mathbf{b} + \phi)V) + \left(\frac{I - I^*}{I}\right)(\phi V - (\mu_0 + \delta + \psi)I) + \left(\frac{R - R^*}{R}\right) \\ &\quad \times (\omega V + \psi I - \delta R), \end{aligned}$$

and setting $S = S - S^*, E = E - E^*, V = V - V^*, I = I - I^*$ and $R = R - R^*$ results in

$$\begin{aligned} D_t^{\xi,\lambda} L &= \mathbf{a} - \mathbf{a}\frac{S^*}{S} - (\delta + \rho + \rho_1)\frac{(S - S^*)^2}{S} + (\rho + \rho_1)S - (\rho + \rho_1)S^* - (\rho + \rho_1)S\frac{E^*}{E} + (\rho + \rho_1)S^*\frac{E^*}{E} \\ &\quad -\delta\frac{(E - E^*)^2}{E} - \rho_2 \alpha V \frac{(E - E^*)^2}{E} + \rho_2 \alpha V^* \frac{(E - E^*)^2}{E} + \rho_2 \alpha E \frac{(V - V^*)^2}{V} - \rho_2 \alpha E^* \frac{(V - V^*)^2}{V} \\ &\quad +\mathbf{b}\frac{(V - V^*)^2}{V} - (\delta + \mu_0 + \omega + \phi)\frac{(V - V^*)^2}{V} + \phi V - \phi V^* - \phi V \frac{I^*}{I} + \phi V^* \frac{I^*}{I} \\ &\quad -(\mu_0 + \delta + \psi)\frac{(I - I^*)^2}{I} + \omega V - \omega V^* - \omega V \frac{R^*}{R} + \omega V^* \frac{R^*}{R} + \psi I - \psi I^* \\ &\quad -\psi I \frac{R^*}{R} + \psi I^* \frac{R^*}{R} - \delta \frac{(R - R^*)^2}{R}. \end{aligned}$$

We can write $D_t^{\xi,\lambda} L = \Sigma - \Omega$, where

$$\begin{aligned} \Sigma &= \mathbf{a} + (\rho + \rho_1)S + (\rho + \rho_1)S^*\frac{E^*}{E} + \rho_2 \alpha V^* \frac{(E - E^*)^2}{E} + \rho_2 \alpha E \frac{(V - V^*)^2}{V} + \mathbf{b}\frac{(V - V^*)^2}{V} + \phi V \\ &\quad +\phi V^* \frac{I^*}{I} + \omega V + \omega V^* \frac{R^*}{R} + \psi I + \psi I^* \frac{R^*}{R}, \end{aligned}$$

and

$$\begin{aligned}\Omega &= \mathbf{a}\frac{S^*}{S} + (\delta+\rho+\rho_1)\frac{(S-S^*)^2}{S} + (\rho+\rho_1)S^* + (\rho+\rho_1)S\frac{E^*}{E} + \delta\frac{(E-E^*)^2}{E} + \rho_2\alpha V\frac{(E-E^*)^2}{E}\\ &+\rho_2\alpha E^*\frac{(V-V^*)^2}{V} + (\delta+\mu_0+\omega+\phi)\frac{(V-V^*)^2}{V} + \phi V^* + \phi V\frac{I^*}{I} + (\mu_0+\delta+\psi)\frac{(I-I^*)^2}{I} + \omega V^*\\ &+\omega V\frac{R^*}{R} + \psi V^* + \psi I\frac{R^*}{R} + \delta\frac{(R-R^*)^2}{R}.\end{aligned}$$

We conclude that if $\Sigma < \Omega$, this yields $D_t^{\xi,\lambda}L < 0$, however when $S = S^*, E = E^*, V = V^*, I = I^*$ and $R = R^*, \Sigma - \Omega = 0 \Rightarrow D_t^{\xi,\lambda}L = 0$.

We can observe that $\left\{(S^*, E^*, V^*, I^*, R^*) \in \Gamma : D_t^{\xi,\lambda}L = 0\right\}$ represents the point D_2 for the developed model.

According to Lasalles' concept of invariance, D_2 is globally uniformly stable in Γ if $\Sigma - \Omega = 0$.

6. Solutions by fractal-fractional operator

Now, we will develop a solution using a numerical approach for our newly developed model given in Eq (2.2). We use the ML kernel in the current scenario instead of the classical derivative operator.

Furthermore, we will use the variable order version.

$$\begin{aligned}{}_0^{FFM}D_t^{\xi,\lambda}S(t) &= \mathbf{a} - (\delta+\rho+\rho_1)S,\\ {}_0^{FFM}D_t^{\xi,\lambda}E(t) &= (\rho+\rho_1)S - \delta E - \rho_2\alpha EV,\\ {}_0^{FFM}D_t^{\xi,\lambda}V(t) &= \rho_2\alpha EV - (\delta+\mu_0+\omega-\mathbf{b}+\phi)V,\\ {}_0^{FFM}D_t^{\xi,\lambda}I(t) &= \phi V - (\mu_0+\delta+\psi)I,\\ {}_0^{FFM}D_t^{\xi,\lambda}R(t) &= \omega V + \psi I - \delta R.\end{aligned}$$

For clarity, we express the above equation as follows:

$$\begin{aligned}{}_0^{FFM}D_t^{\xi,\lambda}S(t) &= S_1(t,S,G),\\ {}_0^{FFM}D_t^{\xi,\lambda}E(t) &= E_1(t,S,G),\\ {}_0^{FFM}D_t^{\xi,\lambda}V(t) &= V_1(t,S,G),\\ {}_0^{FFM}D_t^{\xi,\lambda}I(t) &= I_1(t,S,G),\\ {}_0^{FFM}D_t^{\xi,\lambda}R(t) &= R_1(t,S,G).\end{aligned}$$

Where

$$\begin{aligned}S_1(t,S,G) &= \mathbf{a} - (\delta+\rho+\rho_1)S,\\ E_1(t,S,G) &= (\rho+\rho_1)S - \delta E - \rho_2\alpha EV,\\ V_1(t,S,G) &= \rho_2\alpha EV - (\delta+\mu_0+\omega-\mathbf{b}+\phi)V,\\ I_1(t,S,G) &= \phi V - (\mu_0+\delta+\psi)I,\\ R_1(t,S,G) &= \omega V + \psi I - \delta R.\end{aligned}$$

After using the fractal-fractional integral with the ML kernel, we obtain the following results:

$$\begin{aligned}
S(t_\eta+1) &= \frac{\lambda(1-\xi)}{AB(\xi)}t_\eta^{\lambda-1}S_1\Big(t_\eta,S(t_\eta),G(t_\eta)\Big)\\
&\quad+\frac{\xi\lambda}{AB(\xi)\Gamma(\xi)}\sum_{\nu=2}^{\eta}\int_{t_\nu}^{t_{\nu+1}}S_1(t,S,G)\tau^{\xi-1}(t_{\eta+1}-\tau)^{\xi-1}d\tau,\\
E(t_\eta+1) &= \frac{\lambda(1-\xi)}{AB(\xi)}t_\eta^{\lambda-1}E_1\Big(t_\eta,S(t_\eta),G(t_\eta)\Big)\\
&\quad+\frac{\xi\lambda}{AB(\xi)\Gamma(\xi)}\sum_{\nu=2}^{\eta}\int_{t_\nu}^{t_{\nu+1}}E_1(t,S,G)\tau^{\xi-1}(t_{\eta+1}-\tau)^{\xi-1}d\tau,\\
V(t_\eta+1) &= \frac{\lambda(1-\xi)}{AB(\xi)}t_\eta^{\lambda-1}V_1\Big(t_\eta,S(t_\eta),G(t_\eta)\Big)\\
&\quad+\frac{\xi\lambda}{AB(\xi)\Gamma(\xi)}\sum_{\nu=2}^{\eta}\int_{t_\nu}^{t_{\nu+1}}V_1(t,S,G)\tau^{\xi-1}(t_{\eta+1}-\tau)^{\xi-1}d\tau,\\
I(t_\eta+1) &= \frac{\lambda(1-\xi)}{AB(\xi)}t_\eta^{\lambda-1}I_1\Big(t_\eta,S(t_\eta),G(t_\eta)\Big)\\
&\quad+\frac{\xi\lambda}{AB(\xi)\Gamma(\xi)}\sum_{\nu=2}^{\eta}\int_{t_\nu}^{t_{\nu+1}}I_1(t,S,G)\tau^{\xi-1}(t_{\eta+1}-\tau)^{\xi-1}d\tau,\\
R(t_\eta+1) &= \frac{\lambda(1-\xi)}{AB(\xi)}t_\eta^{\lambda-1}R_1\Big(t_\eta,S(t_\eta),G(t_\eta)\Big)\\
&\quad+\frac{\xi\lambda}{AB(\xi)\Gamma(\xi)}\sum_{\nu=2}^{\eta}\int_{t_\nu}^{t_{\nu+1}}R_1(t,S,G)\tau^{\xi-1}(t_{\eta+1}-\tau)^{\xi-1}d\tau,
\end{aligned}\tag{6.1}$$

where $G(t_\eta)=E(t_\eta),\ V(t_\eta),\ I(t_\eta),\ R(t_\eta)$.

Remember that the Newton polynomial can be obtained by using the Newton interpolation formula.

$$\begin{aligned}
N(t,S,G) &\simeq N(t_{\eta-2},S_{\eta-2},G_{\eta-2})+\frac{1}{\Delta t}\Big[N(t_{\eta-1},S_{\eta-1},G_{\eta-1})\\
&- N(t_{\eta-2},S_{\eta-2},G_{\eta-2})\Big]\Big(\tau-t_{\eta-2}\Big)+\frac{1}{2\Delta t^2}\Big[N(t_\eta,S_\eta,E_\eta,I_\eta,Q_\eta,R_\eta)\\
&- 2N(t_{\eta-1},S_{\eta-1},G_{\eta-1})-N(t_{\eta-2},S_{\eta-2},G_{\eta-2})\Big]\Big(\tau-t_{\eta-2}\Big)\Big(\tau-t_{\eta-1}\Big),
\end{aligned}$$

where $G_{\eta-2}=E_{\eta-2},V_{\eta-2},I_{\eta-2},R_{\eta-2},\quad G_{\eta-1}=E_{\eta-1},V_{\eta-1},I_{\eta-1},R_{\eta-1}$.

When we substitute the Newton polynomial into the system of Eqs (6.1), we obtain the following:

$$\begin{aligned}
S^{\eta+1} &= \frac{\lambda(1-\xi)}{AB(\xi)}t_\eta^{\lambda-1}S_1(t_\eta,S(t_\eta),G(t_\eta))+\frac{\xi\lambda}{AB(\xi)\Gamma(\xi)}\sum_{\nu=2}^{\eta}S_1(t_{\nu-2},S^{\nu-2},G^{\nu-2})\\
&\quad\times t_{\nu-2}^{\lambda-1}\int_{t_\nu}^{t_{\nu+1}}(t_{\eta+1}-\tau)^{\xi-1}d\tau+\frac{\xi\lambda}{AB(\xi)\Gamma(\xi)}\sum_{\nu=2}^{\eta}\frac{1}{\Delta t}\Big[t_{\nu-1}^{\lambda-1}S_1(t_{\nu-1},S^{\nu-1},G^{\nu-1})\\
&\quad-t_{\nu-2}^{\lambda-1}S_1(t_{\nu-2},S^{\nu-2},G^{\nu-2})\Big]\int_{t_\nu}^{t_{\nu+1}}(\tau-t_{\nu-2})(t_{\eta+1}-\tau)^{\xi-1}d\tau
\end{aligned}$$

$$
\begin{aligned}
&+\frac{\xi\lambda}{AB(\xi)\Gamma(\xi)}\sum_{\nu=2}^{\eta}\frac{1}{2\Delta t^2}\Big[t_{\nu}^{\lambda-1}S_1(t_\nu,S^\nu,G^\nu)-2t_{\nu-1}^{\lambda-1}S_1(t_{\nu-1},S^{\nu-1},G^{\nu-1})\\
&+t_{\nu-2}^{\lambda-1}S_1(t_{\nu-2},S^{\nu-2},G^{\nu-2})\Big]\int_{t_\nu}^{t_{\nu+1}}(\tau-t_{\nu-2})(\tau-t_{\nu-1})(t_{\eta+1}-\tau)^{\xi-1}d\tau.\\
E^{\eta+1} &= \frac{\lambda(1-\xi)}{AB(\xi)}t_{\eta}^{\lambda-1}E_1(t_\eta,S(t_\eta),G(t_\eta))+\frac{\xi\lambda}{AB(\xi)\Gamma(\xi)}\sum_{\nu=2}^{\eta}E_1(t_{\nu-2},S^{\nu-2},G^{\nu-2})\\
&\times t_{\nu-2}^{\lambda-1}\int_{t_\nu}^{t_{\nu+1}}(t_{\eta+1}-\tau)^{\xi-1}d\tau\ +\frac{\xi\lambda}{AB(\xi)\Gamma(\xi)}\sum_{\nu=2}^{\eta}\frac{1}{\Delta t}\Big[t_{\nu-1}^{\lambda-1}E_1(t_{\nu-1},S^{\nu-1},G^{\nu-1})\\
&-t_{\nu-2}^{\lambda-1}E_1(t_{\nu-2},S^{\nu-2},G^{\nu-2})\Big]\int_{t_\nu}^{t_{\nu+1}}(\tau-t_{\nu-2})(t_{\eta+1}-\tau)^{\xi-1}d\tau\\
&+\frac{\xi\lambda}{AB(\xi)\Gamma(\xi)}\sum_{\nu=2}^{\eta}\frac{1}{2\Delta t^2}\Big[t_{\nu}^{\lambda-1}E_1(t_\nu,S^\nu,G^\nu)-2t_{\nu-1}^{\lambda-1}E_1(t_{\nu-1},S^{\nu-1},G^{\nu-1})\\
&+t_{\nu-2}^{\lambda-1}E_1(t_{\nu-2},S^{\nu-2},G^{\nu-2})\Big]\int_{t_\nu}^{t_{\nu+1}}(\tau-t_{\nu-2})(\tau-t_{\nu-1})(t_{\eta+1}-\tau)^{\xi-1}d\tau.\\
V^{\eta+1} &= \frac{\lambda(1-\xi)}{AB(\xi)}t_{\eta}^{\lambda-1}V_1(t_\eta,S(t_\eta),G(t_\eta))+\frac{\xi\lambda}{AB(\xi)\Gamma(\xi)}\sum_{\nu=2}^{\eta}V_1(t_{\nu-2},S^{\nu-2},G^{\nu-2})\\
&\times t_{\nu-2}^{\lambda-1}\int_{t_\nu}^{t_{\nu+1}}(t_{\eta+1}-\tau)^{\xi-1}d\tau+\frac{\xi\lambda}{AB(\xi)\Gamma(\xi)}\sum_{\nu=2}^{\eta}\frac{1}{\Delta t}\Big[t_{\nu-1}^{\lambda-1}V_1(t_{\nu-1},S^{\nu-1},G^{\nu-1})\\
&-t_{\nu-2}^{\lambda-1}V_1(t_{\nu-2},S^{\nu-2},G^{\nu-2})\Big]\int_{t_\nu}^{t_{\nu+1}}(\tau-t_{\nu-2})(t_{\eta+1}-\tau)^{\xi-1}d\tau\\
&+\frac{\xi\lambda}{AB(\xi)\Gamma(\xi)}\sum_{\nu=2}^{\eta}\frac{1}{2\Delta t^2}\Big[t_{\nu}^{\lambda-1}V_1(t_\nu,S^\nu,G^\nu)-2t_{\nu-1}^{\lambda-1}V_1(t_{\nu-1},S^{\nu-1},G^{\nu-1})\\
&+t_{\nu-2}^{\lambda-1}V_1(t_{\nu-2},S^{\nu-2},G^{\nu-2})\Big]\int_{t_\nu}^{t_{\nu+1}}(\tau-t_{\nu-2})(\tau-t_{\nu-1})(t_{\eta+1}-\tau)^{\xi-1}d\tau. \qquad (6.2)\\
I^{\eta+1} &= \frac{\lambda(1-\xi)}{AB(\xi)}t_{\eta}^{\lambda-1}I_1(t_\eta,S(t_\eta),G(t_\eta))+\frac{\xi\lambda}{AB(\xi)\Gamma(\xi)}\sum_{\nu=2}^{\eta}I_1(t_{\nu-2},S^{\nu-2},G^{\nu-2})\\
&\times t_{\nu-2}^{\lambda-1}\int_{t_\nu}^{t_{\nu+1}}(t_{\eta+1}-\tau)^{\xi-1}d\tau+\frac{\xi\lambda}{AB(\xi)\Gamma(\xi)}\sum_{\nu=2}^{\eta}\frac{1}{\Delta t}\Big[t_{\nu-1}^{\lambda-1}I_1(t_{\nu-1},S^{\nu-1},G^{\nu-1})\\
&-t_{\nu-2}^{\lambda-1}I_1(t_{\nu-2},S^{\nu-2},G^{\nu-2})\Big]\int_{t_\nu}^{t_{\nu+1}}(\tau-t_{\nu-2})(t_{\eta+1}-\tau)^{\xi-1}d\tau\\
&+\frac{\xi\lambda}{AB(\xi)\Gamma(\xi)}\sum_{\nu=2}^{\eta}\frac{1}{2\Delta t^2}\Big[t_{\nu}^{\lambda-1}I_1(t_\nu,S^\nu,G^\nu)-2t_{\nu-1}^{\lambda-1}Q_1(t_{\nu-1},S^{\nu-1},G^{\nu-1})\\
&+t_{\nu-2}^{\lambda-1}I_1(t_{\nu-2},S^{\nu-2},G^{\nu-2})\Big]\int_{t_\nu}^{t_{\nu+1}}(\tau-t_{\nu-2})(\tau-t_{\nu-1})(t_{\eta+1}-\tau)^{\xi-1}d\tau.
\end{aligned}
$$

$$
\begin{aligned}
R^{\eta+1} &= \frac{\lambda(1-\xi)}{AB(\xi)} t_\eta^{\lambda-1} R_1(t_\eta, S(t_\eta), G(t_\eta)) + \frac{\xi\lambda}{AB(\xi)\Gamma(\xi)} \sum_{\nu=2}^{\eta} R_1(t_{\nu-2}, S^{\nu-2}, G^{\nu-2}) \\
&\times t_{\nu-2}^{\lambda-1} \int_{t_\nu}^{t_{\nu+1}} (t_{\eta+1}-\tau)^{\xi-1} d\tau + \frac{\xi\lambda}{AB(\xi)\Gamma(\xi)} \sum_{\nu=2}^{\eta} \frac{1}{\Delta t} \Big[t_{\nu-1}^{\lambda-1} R_1(t_{\nu-1}, S^{\nu-1}, G^{\nu-1}) \\
&- t_{\nu-2}^{\lambda-1} R_1(t_{\nu-2}, S^{\nu-2}, G^{\nu-2}) \Big] \int_{t_\nu}^{t_{\nu+1}} (\tau - t_{\nu-2})(t_{\eta+1}-\tau)^{\xi-1} d\tau \\
&+ \frac{\xi\lambda}{AB(\xi)\Gamma(\xi)} \sum_{\nu=2}^{\eta} \frac{1}{2\Delta t^2} \Big[t_\nu^{\lambda-1} R_1(t_\nu, S^\nu, G^\nu) - 2t_{\nu-1}^{\lambda-1} R_1(t_{\nu-1}, S^{\nu-1}, G^{\nu-1}) \\
&+ t_{\nu-2}^{\lambda-1} R_1(t_{\nu-2}, S^{\nu-2}, G^{\nu-2}) \Big] \int_{t_\nu}^{t_{\nu+1}} (\tau - t_{\nu-2})(\tau - t_{\nu-1})(t_{\eta+1}-\tau)^{\xi-1} d\tau,
\end{aligned}
$$

where $G^{\nu-2} = E^{\nu-2}, V^{\nu-2}, I^{\nu-2}, R^{\nu-2}$, $G^{\nu-1} = E^{\nu-1}, V^{\nu-1}, I^{\nu-1}, R^{\nu-1}$, $G^{\nu} = E^{\nu}, V^{\nu}, I^{\nu}, R^{\nu}$, and $G(t_\eta) = E(t_\eta), V(t_\eta), I(t_\eta), R(t_\eta)$.

We can perform the following calculations for the integral in Eq (6.2):

$$
\begin{aligned}
\int_{t_\nu}^{t_{\nu+1}} (t_{\eta+1}-\tau)^{\xi-1} d\tau &= \frac{(\Delta t)^\xi}{\xi} \Big[(\eta-\nu+1)^\xi - (\eta-\nu)^\xi \Big], \\
\int_{t_\nu}^{t_{\nu+1}} (\tau - t_{\nu-2})(t_{\eta+1}-\tau)^{\xi-1} d\tau &= \frac{(\Delta t)^{\xi+1}}{\xi(\xi+1)} \Big[(\eta-\nu+1)^\xi \\
&\times (\eta-\nu+3+2\xi) - (\eta-\nu)^\xi (\eta-\nu+3+3\xi) \Big]. \qquad (6.3) \\
\int_{t_\nu}^{t_{\nu+1}} (\tau - t_{\nu-2})(\tau - t_{\nu-1})(t_{\eta+1}-\tau)^{\xi-1} d\tau &= \frac{(\Delta t)^{\xi+2}}{\xi(\xi+1)(\xi+2)} \Big[(\eta-\nu+1)^\xi \Big\{ 2(\eta-\nu)^2 + (3\xi+10) \\
&\times (\eta-\nu) + 2\xi^2 + 9\xi + 12 \Big\} - (\eta-\nu)^\xi \Big\{ 2(\eta-\nu)^2 \\
&+ (5\xi+10)(\eta-\nu) + 6\xi^2 + 18\xi + 12 \Big\} \Big],
\end{aligned}
$$

substituting integral calculation values into Eq (6.2).

We acquire the numerical solutions $S(t), E(t), V(t), I(t)$ *and* $R(t)$:

$$
\begin{aligned}
S^{\eta+1} &= \frac{\lambda(1-\xi)}{AB(\xi)} t_\eta^{\lambda-1} S_1(t_\eta, S(t_\eta), G(t_\eta)) + \frac{\xi\lambda(\Delta t)^\xi}{AB(\xi)\Gamma(\xi+1)} \sum_{\nu=2}^{\eta} S_1(t_{\nu-2}, S^{\nu-2}, G^{\nu-2}) \\
&\times t_{\nu-2}^{\lambda-1} \Big[(\eta-\nu+1)^\xi - (\eta-\nu)^\xi \Big] + \frac{\xi\lambda(\Delta t)^\xi}{AB(\xi)\Gamma(\xi+2)} \sum_{\nu=2}^{\eta} \Big[t_{\nu-1}^{\lambda-1} S_1(t_{\nu-1}, S^{\nu-1}, G^{\nu-1}) \\
&- t_{\nu-2}^{\lambda-1} S_1(t_{\nu-2}, S^{\nu-2}, G^{\nu-2}) \Big] \Big[(\eta-\nu+1)^\xi (\eta-\nu+3+2\xi) - (\eta-\nu)^\xi (\eta-\nu+3+3\xi) \Big] \\
&+ \frac{\xi\lambda(\Delta t)^\xi}{2AB(\xi)\Gamma(\xi+3)} \sum_{\nu=2}^{\eta} \Big[t_\nu^{\lambda-1} S_1(t_\nu, S^\nu, G^\nu) - 2t_{\nu-1}^{\lambda-1} S_1(t_{\nu-1}, S^{\nu-1}, G^{\nu-1}) \\
&+ t_{\nu-2}^{\lambda-1} S_1(t_{\nu-2}, S^{\nu-2}, G^{\nu-2}) \Big] \Big[(\eta-\nu+1)^\xi \Big\{ 2(\eta-\nu)^2 + (3\xi+10)(\eta-\nu) + 2\xi^2 + 9\xi + 12 \Big\} \\
&- (\eta-\nu)^\xi \times \Big\{ 2(\eta-\nu)^2 + (5\xi+10)(\eta-\nu) + 6\xi^2 + 18\xi + 12 \Big\} \Big],
\end{aligned}
$$

$$
\begin{aligned}
E^{\eta+1} &= \frac{\lambda(1-\xi)}{AB(\xi)} t_{\eta}^{\lambda-1} E_1(t_\eta, S(t_\eta), G(t_\eta)) + \frac{\xi\lambda(\Delta t)^{\xi}}{AB(\xi)\Gamma(\xi+1)} \sum_{\nu=2}^{\eta} E_1(t_{\nu-2}, S^{\nu-2}, G^{\nu-2}) \\
&\times t_{\nu-2}^{\lambda-1}\Big[(\eta-\nu+1)^{\xi} - (\eta-\nu)^{\xi}\Big] + \frac{\xi\lambda(\Delta t)^{\xi}}{AB(\xi)\Gamma(\xi+2)} \sum_{\nu=2}^{\eta} \Big[t_{\nu-1}^{\lambda-1} E_1(t_{\nu-1}, S^{\nu-1}, G^{\nu-1}) \\
&- t_{\nu-2}^{\lambda-1} E_1(t_{\nu-2}, S^{\nu-2}, G^{\nu-2})\Big]\Big[(\eta-\nu+1)^{\xi}(\eta-\nu+3+2\xi) - (\eta-\nu)^{\xi}(\eta-\nu+3+3\xi)\Big] \\
&+ \frac{\xi\lambda(\Delta t)^{\xi}}{2AB(\xi)\Gamma(\xi+3)} \sum_{\nu=2}^{\eta} \Big[t_{\nu}^{\lambda-1} E_1(t_\nu, S^{\nu}, G^{\nu}) - 2t_{\nu-1}^{\lambda-1} E_1(t_{\nu-1}, S^{\nu-1}, G^{\nu-1}) \\
&+ t_{\nu-2}^{\lambda-1} E_1(t_{\nu-2}, S^{\nu-2}, G^{\nu-2})\Big]\Big[(\eta-\nu+1)^{\xi}\Big\{2(\eta-\nu)^2 + (3\xi+10)(\eta-\nu) + 2\xi^2 + 9\xi + 12\Big\} \\
&- (\eta-\nu)^{\xi} \times \Big\{2(\eta-\nu)^2 + (5\xi+10)(\eta-\nu) + 6\xi^2 + 18\xi + 12\Big\}\Big], \\
V^{\eta+1} &= \frac{\lambda(1-\xi)}{AB(\xi)} t_{\eta}^{\lambda-1} V_1(t_\eta, S(t_\eta), G(t_\eta)) + \frac{\xi\lambda(\Delta t)^{\xi}}{AB(\xi)\Gamma(\xi+1)} \sum_{\nu=2}^{\eta} V_1(t_{\nu-2}, S^{\nu-2}, G^{\nu-2}) \\
&\times t_{\nu-2}^{\lambda-1}\Big[(\eta-\nu+1)^{\xi} - (\eta-\nu)^{\xi}\Big] + \frac{\xi\lambda(\Delta t)^{\xi}}{AB(\xi)\Gamma(\xi+2)} \sum_{\nu=2}^{\eta} \Big[t_{\nu-1}^{\lambda-1} V_1(t_{\nu-1}, S^{\nu-1}, G^{\nu-1}) \\
&- t_{\nu-2}^{\lambda-1} V_1(t_{\nu-2}, S^{\nu-2}, G^{\nu-2})\Big]\Big[(\eta-\nu+1)^{\xi}(\eta-\nu+3+2\xi) - (\eta-\nu)^{\xi}(\eta-\nu+3+3\xi)\Big] \\
&+ \frac{\xi\lambda(\Delta t)^{\xi}}{2AB(\xi)\Gamma(\xi+3)} \sum_{\nu=2}^{\eta} \Big[t_{\nu}^{\lambda-1} V_1(t_\nu, S^{\nu}, G^{\nu}) - 2t_{\nu-1}^{\lambda-1} V_1(t_{\nu-1}, S^{\nu-1}, G^{\nu-1}) \\
&+ t_{\nu-2}^{\lambda-1} V_1(t_{\nu-2}, S^{\nu-2}, G^{\nu-2})\Big]\Big[(\eta-\nu+1)^{\xi}\Big\{2(\eta-\nu)^2 + (3\xi+10)(\eta-\nu) + 2\xi^2 + 9\xi + 12\Big\} \\
&- (\eta-\nu)^{\xi} \times \Big\{2(\eta-\nu)^2 + (5\xi+10)(\eta-\nu) + 6\xi^2 + 18\xi + 12\Big\}\Big], \\
I^{\eta+1} &= \frac{\lambda(1-\xi)}{AB(\xi)} t_{\eta}^{\lambda-1} I_1(t_\eta, S(t_\eta), G(t_\eta)) + \frac{\xi\lambda(\Delta t)^{\xi}}{AB(\xi)\Gamma(\xi+1)} \sum_{\nu=2}^{\eta} I_1(t_{\nu-2}, S^{\nu-2}, G^{\nu-2}) \\
&\times t_{\nu-2}^{\lambda-1}\Big[(\eta-\nu+1)^{\xi} - (\eta-\nu)^{\xi}\Big] + \frac{\xi\lambda(\Delta t)^{\xi}}{AB(\xi)\Gamma(\xi+2)} \sum_{\nu=2}^{\eta} \Big[t_{\nu-1}^{\lambda-1} I_1(t_{\nu-1}, S^{\nu-1}, G^{\nu-1}) \\
&- t_{\nu-2}^{\lambda-1} I_1(t_{\nu-2}, S^{\nu-2}, G^{\nu-2})\Big]\Big[(\eta-\nu+1)^{\xi}(\eta-\nu+3+2\xi) - (\eta-\nu)^{\xi}(\eta-\nu+3+3\xi)\Big] \\
&+ \frac{\xi\lambda(\Delta t)^{\xi}}{2AB(\xi)\Gamma(\xi+3)} \sum_{\nu=2}^{\eta} \Big[t_{\nu}^{\lambda-1} I_1(t_\nu, S^{\nu}, G^{\nu}) - 2t_{\nu-1}^{\lambda-1} I_1(t_{\nu-1}, S^{\nu-1}, G^{\nu-1}) \\
&+ t_{\nu-2}^{\lambda-1} I_1(t_{\nu-2}, S^{\nu-2}, G^{\nu-2})\Big]\Big[(\eta-\nu+1)^{\xi}\Big\{2(\eta-\nu)^2 + (3\xi+10)(\eta-\nu) + 2\xi^2 + 9\xi + 12\Big\} \\
&- (\eta-\nu)^{\xi} \times \Big\{2(\eta-\nu)^2 + (5\xi+10)(\eta-\nu) + 6\xi^2 + 18\xi + 12\Big\}\Big], \\
R^{\eta+1} &= \frac{\lambda(1-\xi)}{AB(\xi)} t_{\eta}^{\lambda-1} R_1(t_\eta, S(t_\eta), G(t_\eta)) + \frac{\xi\lambda(\Delta t)^{\xi}}{AB(\xi)\Gamma(\xi+1)} \sum_{\nu=2}^{\eta} R_1(t_{\nu-2}, S^{\nu-2}, G^{\nu-2}) \\
&\times t_{\nu-2}^{\lambda-1}\Big[(\eta-\nu+1)^{\xi} - (\eta-\nu)^{\xi}\Big] + \frac{\xi\lambda(\Delta t)^{\xi}}{AB(\xi)\Gamma(\xi+2)} \sum_{\nu=2}^{\eta} \Big[t_{\nu-1}^{\lambda-1} R_1(t_{\nu-1}, S^{\nu-1}, G^{\nu-1}) \\
&- t_{\nu-2}^{\lambda-1} R_1(t_{\nu-2}, S^{\nu-2}, G^{\nu-2})\Big]\Big[(\eta-\nu+1)^{\xi}(\eta-\nu+3+2\xi) - (\eta-\nu)^{\xi}(\eta-\nu+3+3\xi)\Big]
\end{aligned}
$$

$$+\frac{\xi\lambda(\Delta t)^{\xi}}{2AB(\xi)\Gamma(\xi+3)}\sum_{\nu=2}^{\eta}\Big[t_{\nu}^{\lambda-1}R_1(t_{\nu},S^{\nu},G^{\nu})-2t_{\nu-1}^{\lambda-1}R_1(t_{\nu-1},S^{\nu-1},G^{\nu-1})$$
$$+t_{\nu-2}^{\lambda-1}R_1(t_{\nu-2},S^{\nu-2},G^{\nu-2})\Big]\Big[(\eta-\nu+1)^{\xi}\Big\{2(\eta-\nu)^2+(3\xi+10)(\eta-\nu)+2\xi^2+9\xi+12\Big\}$$
$$-(\eta-\nu)^{\xi}\times\Big\{2(\eta-\nu)^2+(5\xi+10)(\eta-\nu)+6\xi^2+18\xi+12\Big\}\Big].$$

7. Simulation explanation

In this section, we utilized an advanced technique to obtain theoretical outcomes and assess their effectiveness. The newly developed SEVIR system was analyzed through simulation. By applying non-integer parametric values in the SARS-COVID-19 model, we obtained interesting findings. Figures 2–6 display the solutions for $S(t)$, $E(t)$, $V(t)$, $I(t)$, and $R(t)$ by reducing the fractional values to the desired level. To validate the efficiency of the theoretical outcomes, we provide the following examples. Numerical simulations for the SARS-COVID-19 model were performed using MATLAB. The initial conditions used in the newly developed model are $S(0) = 217.342565, E(0) = 100, V(0) = 1.386348, I(0) = 1.1$ and $R(0) = 1.271087$. The parameter values used in the developed system are as follows: $\mathbf{a} = 1.43$, $\delta = 0.000065$, $\rho = 0.45$, $\rho_1 = 0.10$, $\rho_2 = 0.020$, $\alpha = 0.0008601$, $\mu_0 = 0.19$, $\omega = 0.98$, $\mathbf{b} = 0.135$, $\phi = 0.0001$, and $\psi = 0.0001$. Figures 2, 4, and 5 illustrate the changes in susceptible, vaccinated, and infected individuals respectively, showing a sharp decrease before reaching a stable position. Meanwhile, Figures 3 and 6 demonstrate the dynamics of exposed and recovered individuals respectively at different fractional orders in which both individuals increases and after certain time the number of individuals approaches stable state using different dimensions. The research predicts future infection rates and suggests ways to decrease the spread of infection units more effectively. By utilizing a fractal-fractional approach, the study yields reliable and accurate results for all compartments at non-integer order derivatives, which are more trustworthy when fractional values are reduced as well a by reducing its dimensions. The findings suggest that the number of infected individuals decreases significantly due to vaccination measures, while the number of recovered individuals increases due to a decline in infected individuals and the effect of vaccination.

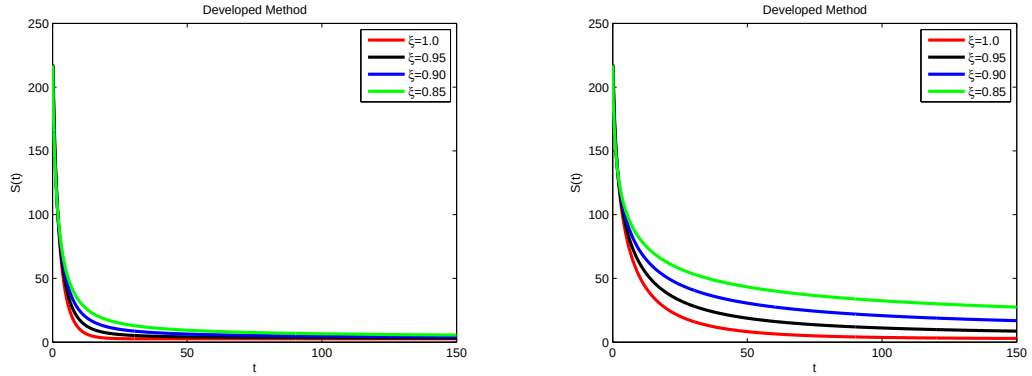

(a) with dimension 0.8 **(b)** with dimension 0.5

Figure 2. The value of $S(t)$ using the fractal-fractional operator with various fractional values at different dimensions.

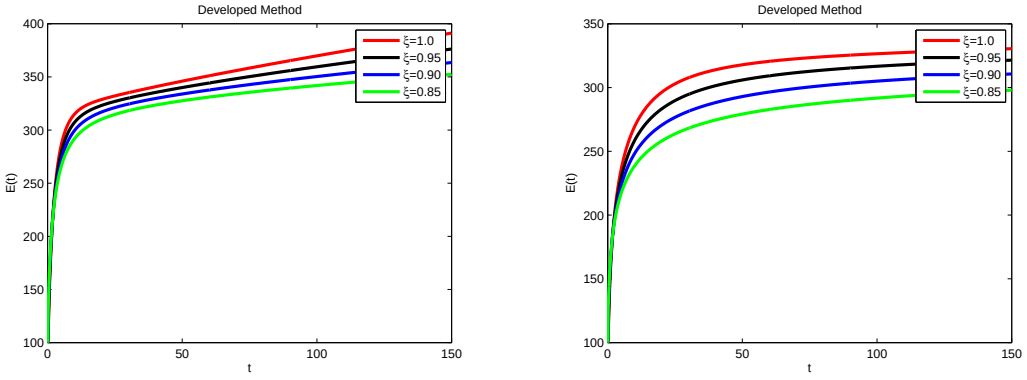

(a) with dimension 0.8 **(b)** with dimension 0.5

Figure 3. The value of $E(t)$ using the fractal-fractional operator with various fractional values at different dimensions.

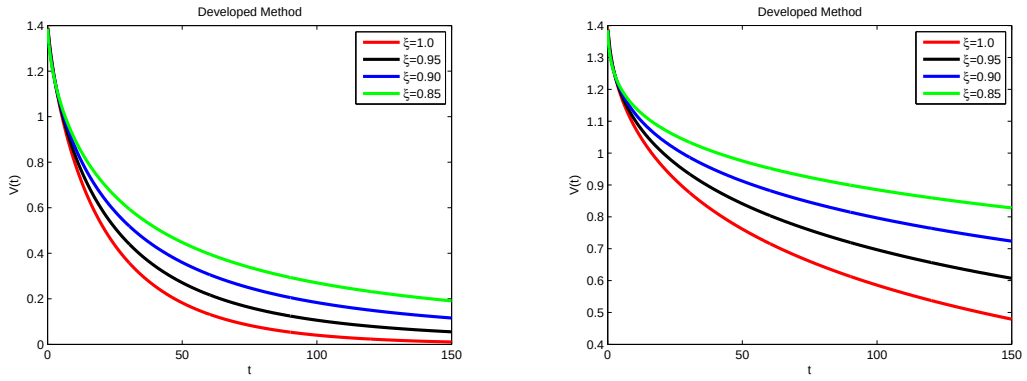

(a) with dimension 0.8 **(b)** with dimension 0.5

Figure 4. The value of $V(t)$ using the fractal-fractional operator with various fractional values at different dimensions.

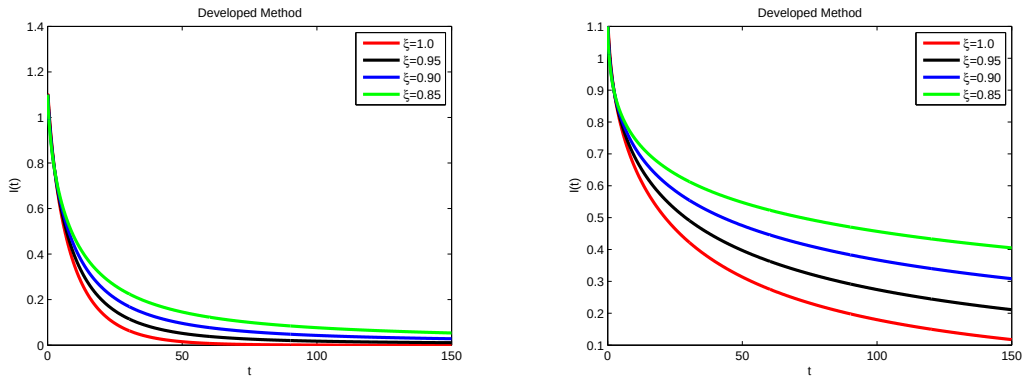

(a) with dimension 0.8 **(b)** with dimension 0.5

Figure 5. The value of $I(t)$ using the fractal-fractional operator with various fractional values at different dimensions.

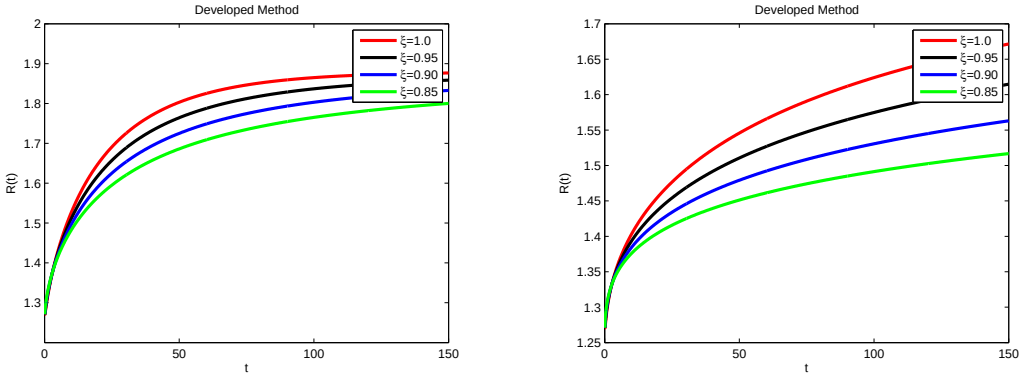

(a) with dimension 0.8 **(b)** with dimension 0.5

Figure 6. The value of $R(t)$ using the fractal-fractional operator with various fractional values at different dimensions.

8. Conclusions

This article employs a fractional order SEVIR model for SARS-COVID-19 with vaccinated effects using an FFO to find reliable solutions. We provide advice on controlling this virus to help our community overcome the pandemic by implementing vaccinated measures for low immune individuals. We analyze the dangerous coronavirus disease with the effect of vaccination to understand its real impact on the community. Qualitative and quantitative analyses are conducted to verify its stable position in a continuous dynamical system. We also verify that the fractional order coronavirus disease model has bounded and unique solutions. We examine the impact of global measures to control the spread of the coronavirus disease. Also, analyses are performed to see how the rate of infection changes after the implementation of vaccination measures. We ensure that our findings are reliable and realistic. FFO is used for continuously monitoring the spread as well as control of the disease in society after vaccination measures. It was observed that infected individuals recover quickly due to the vaccinated strategy. The fractal-fractional operator (FFO) is used for continuously monitoring for the spread of the diseases using different fractional values as well as reliable solutions. In fractal-fractional operators, fractal represents the dimensions of the spread of the disease, and fractional represents the fractional ordered derivative operator which provides the real behavior of the spread as well as control of COVID-19 with different dimensions and continuous monitoring, which can be observed in simulation. We conduct numerical simulations to observe how the disease controlled in the community after the implementation of vaccination measures using different fractional values with different dimensions. Additionally, future estimates are provided based on our findings, which can help in mitigating the risk of the disease spreading in the environment.

Use of AI tools declaration

The authors declare they have not used Artificial Intelligence (AI) tools in the creation of this article.

Acknowledgments

The authors would like to extend their sincere appreciation to Researchers Supporting Project number (RSP2024R472), King Saud University, Riyadh, Saudi Arabia.

Conflict of interest

All authors declare no conflicts of interest in this paper.

References

1. I. Podlubny, *Fractional differential equations: An introduction to fractional derivatives, fractional differential equations, to methods of their solution and some of their applications*, San Diego: Academic Press, 1999.
2. A. Atangana, Non validity of index law in fractional calculus: A fractional differential operator with Markovian and non-Markovian properties, *Physica A*, **505** (2018), 688–706. https://doi.org/10.1016/j.physa.2018.03.056
3. A. K. Golmankhaneh, C. Tunç, Sumudu transform in fractal calculus, *Appl. Math. Comput.*, **350** (2019), 386–401. https://doi.org/10.1016/j.amc.2019.01.025
4. M. Goyal, H. M. Baskonus, A. Prakash, An efficient technique for a time fractional model of lassa hemorrhagic fever spreading in pregnant women, *Eur. Phys. J. Plus*, **134** (2019), 482. https://doi.org/10.1140/epjp/i2019-12854-0
5. I. Nesteruk, Statistics based predictions of coronavirus 2019-nCoV spreading in mainland China, *Innovative Biosyst. Bioeng.*, **4** (2020), 13–18. https://doi.org/10.20535/ibb.2020.4.1.195074
6. K. Shah, R. U. Din, W. Deebani, P. Kumam, Z. Shah, On nonlinear classical and fractional order dynamical system addressing COVID-19, *Results Phys.*, **24** (2021), 104069. https://doi.org/10.1016/j.rinp.2021.104069
7. A. J. Lotka, Contribution to the theory of periodic reactions, *J. Phys. Chem.*, **14** (1910), 271–274. https://doi.org/10.1021/j150111a004
8. N. S. Goel, S. C. Maitra, E. W. Montroll, On the Volterra and other nonlinear models of interacting populations, *Rev. Mod. Phys.*, **43** (1971), 231. https://doi.org/10.1103/RevModPhys.43.231
9. M. M. Khalsaraei, An improvement on the positivity results for 2-stage explicit Runge-Kutta methods, *J. Comput. Appl. Math.*, **235** (2010), 137–143. https://doi.org/10.1016/j.cam.2010.05.020
10. P. Zhou, X. L. Yang, X. G. Wang, B. Hu, L. Zhang, W. Zhang, et al., A pneumonia outbreak associated with a new coronavirus of probable bat origin, *Nature*, **579** (2020), 270–273. https://doi.org/10.1038/s41586-020-2012-7
11. Q. Li, X. Guan, P. Wu, X. Wang, L. Zhou, Y. Tong, et al., Early transmission dynamics in Wuhan, China, of novel coronavirus infected pneumonia, *N. Engl. J. Med.*, **382** (2020), 1199–1207. https://doi.org/10.1056/NEJMoa2001316

12. I. I. Bogoch, A. Watts, A. Thomas-Bachli, C. Huber, M. U. Kraemer, K. Khan, Pneumonia of unknown aetiology in Wuhan, China: Potential for international spread via commercial air travel, *J. Travel Med.*, **27** (2020), taaa008. https://doi.org/10.1093/jtm/taaa008

13. A. B. Gumel, S. Ruan, T. Day, J. Watmough, F. Brauer, P. Van den Driessche, et al., Modelling strategies for controlling SARS out breaks, *Proc. R. Soc. Lond. B*, **271** (2004), 2223–2232. https://doi.org/10.1098/rspb.2004.2800

14. R. Kahn, I. Holmdahl, S. Reddy, J. Jernigan, M. J. Mina, R. B. Slayton, Mathematical modeling to inform vaccination strategies and testing approaches for coronavirus disease 2019 (COVID-19) in nursing homes, *Clin. Infect. Dis.*, **74** (2022), 597–603. https://doi.org/10.1093/cid/ciab517

15. J. Mondal, S. Khajanchi, Mathematical modeling and optimal intervention strategies of the COVID-19 outbreak, *Nonlinear Dyn.*, **109** (2022), 177–202. https://doi.org/10.1007/s11071-022-07235-7

16. S. Hussain, E. N. Madi, H. Khan, H. Gulzar, S. Etemad, S. Rezapour, et al., On the stochastic modeling of COVID-19 under the environmental white noise, *J. Funct. Space*, **2022** (2022), 4320865. https://doi.org/10.1155/2022/4320865

17. WHO, *Statement on the second meeting of the international health regulations emergency committee regarding the outbreak of novel coronavirus (2019-nCoV)*, 2020.

18. J. Page, D. Hinshaw, B. McKay, In hunt for COVID-19 origin, patient zero points to second Wuhan market - the man with the first confirmed infection of the new coronavirus told the WHO team that his parents had shopped there, In: *The Wall Street Journal*, 2021.

19. S. Zhao, H. Chen, Modeling the epidemic dynamics and control of covid-19 outbreak in China, *Quant. Biol.*, **8** (2020), 11–19. https://doi.org/10.1007/s40484-020-0199-0

20. C. Rivers, J. P. Chretien, S. Riley, J. A. Pavlin, A. Woodward, D. Brett-Major, et al., Using "outbreak science" to strengthen the use of models during epidemics, *Nat. Commun.*, **10** (2019), 3102. https://doi.org/10.1038/s41467-019-11067-2

21. K. Sun, J. Chen, C. Viboud, Early epidemiological analysis of the coronavirus disease 2019 outbreak based on crowd sourced data: A population-level observational study, *Lancet Digital Health*, **2** (2020), e201–e208. https://doi.org/10.1016/S2589-7500(20)30026-1

22. N. Zhu, D. Zhang, W. Wang, X. Li, B. Yang, J. Song, et al., A novel coronavirus from patients with pneumonia in China, 2019, *N. Engl. J. Med.*, **382** (2020), 727–733. https://doi.org/10.1056/NEJMoa2001017

23. N. M. Linton, T. Kobayashi, Y. Yang, K. Hayashi, A. R. Akhmetzhanov, S. M. Jung, et al., Incubation period and other epidemiological characteristics of 2019 novel coronavirus infections with right truncation: A statistical analysis of publicly available case data, *J. Clin. Med.*, **9** (2020), 538. https://doi.org/10.3390/jcm9020538

24. C. Huang, Y. Wang, X. Li, L. Ren, J. Zhao Y. Hu, et al., Clinical features of patients infected with 2019 novel coronavirus in Wuhan, China, *Lancet*, **395** (2020), 497–506. https://doi.org/10.1016/S0140-6736(20)30183-5

25. C. A. Donnelly, A. C. Ghani, G. M. Leung, A. J. Hedley, C. Fraser, S. Riley, et al., Epidemiological determinants of spread of causal agent of severe acute respiratory syndrome in Hong Kong, *Lancet*, **361** (2003), 1761–1766. https://doi.org/10.1016/S0140-6736(03)13410-1

26. S. Ullah, M. A. Khan, M. Farooq, Z. Hammouch, D. Baleanu, A fractional model for the dynamics of tuberculosis infection using caputo-fabrizio derivative, *Discrete Contin. Dyn. Syst. S*, **13** (2020), 975–993. https://doi.org/10.3934/dcdss.2020057

27. M. A. Khan, A. Atangana, Modeling the dynamics of novel coronavirus (2019-nCoV) with fractional derivative, *Alex. Eng. J.*, **59** (2020), 2379–2389. http://dx.doi.org/10.1016/j.aej.2020.02.033

28. M. Rahman, M. Arfan, K. Shah, J. F. Gómez-Aguilar, Investigating a nonlinear dynamical model of COVID-19 disease under fuzzy caputo, random and ABC fractional order derivative, *Chaos Soliton Fract.*, **140** (2020), 110232. https://doi.org/10.1016/j.chaos.2020.110232

29. M. Farman, A. Ahmad, A. Akgül, M. U. Saleem, K. S. Nisar, V. Vijayakumar, Dynamical behavior of tumor-immune system with fractal-fractional operator, *AIMS Mathematics*, **7** (2022), 8751–8773. https://doi.org/10.3934/math.2022489

30. K. S. Nisar, A. Ahmad, M. Inc, M. Farman, H. Rezazadeh, L. Akinyemi, et al., Analysis of dengue transmission using fractional order scheme, *AIMS Mathematics*, **7** (2022), 8408–8429. https://doi.org/10.3934/math.2022469

31. M. Farman, M. Amin, A. Akgül, A. Ahmad, M. B. Riaz, S. Ahmad, Fractal-fractional operator for COVID-19 (Omicron) variant outbreak with analysis and modeling, *Results Phys.*, **39** (2022), 105630. https://doi.org/10.1016/j.rinp.2022.105630

32. A. Ahmad, Q. M. Farooq, H. Ahmad, D. U. Ozsahin, F. Tchier, A. Ghaffar, et al., Study on symptomatic and asymptomatic transmissions of COVID-19 including flip bifurcation, *Int. J. Biomath.*, **20** (2024), 699–717. https://doi.org/10.1142/S1793524524500025

33. A. Ahmad, C. Alfiniyah, A. Akgül, A. A. Raezah, Analysis of COVID-19 outbreak in Democratic Republic of the Congo using fractional operators, *AIMS Mathematics*, **8** (2023), 25654–25687. https://doi.org/10.3934/math.20231309

34. N. H. Alharthi, M. B. Jeelani, Analyzing a SEIR-type mathematical model of SARS-COVID-19 using piecewise fractional order operators, *AIMS Mathematics*, **8** (2023), 27009–27032. https://doi.org/10.3934/math.20231382

35. A. Akgül, C. Li, I. Pehlivan, Amplitude control analysis of a four-wing chaotic attractor, its electronic circuit designs and microcontroller-based random number generator, *J. Circuit Syst. Comp.*, **26** (2017), 1750190. https://doi.org/10.1142/S0218126617501900

36. A. Atangana, Mathematical model of survival of fractional calculus, critics and their impact: How singular is our world?, *Adv. Differ. Equ.*, **2021** (2021), 403. https://doi.org/10.1186/s13662-021-03494-7

37. A. Atangana, Modelling the spread of COVID-19 with new fractal-fractional operators: Can the lockdown save mankind before vaccination?, *Chaos Soliton Fract.*, **136** (2020), 109860. https://doi.org/10.1016/j.chaos.2020.109860

38. A. Atangana, S. Iğret Araz, Mathematical model of COVID-19 spread in Turkey and South Africa: Theory, methods, and applications, *Adv. Differ. Equ.*, **2020** (2020), 659. https://doi.org/10.1186/s13662-020-03095-w

39. R. Shi, H. Zhao, S. Tang, Global dynamic analysis of a vector-borne plant disease model, *Adv. Differ. Equ.*, **2014** (2014), 59. https://doi.org/10.1186/1687-1847-2014-59

40. W. Lin, Global existence theory and chaos control of fractional differential equations, *J. Math. Anal. Appl.*, **332** (2007), 709–726. https://doi.org/10.1016/j.jmaa.2006.10.040

41. C. Xu, M. Farman, A. Hasan, A. Akgül, M. Zakarya, W. Albalawi, et al., Lyapunov stability and wave analysis of Covid-19 omicron variant of real data with fractional operator, *Alex. Eng. J.*, **61** (2022), 11787–11802. https://doi.org/10.1016/j.aej.2022.05.025

AIMS Press